

Main revisions and response to reviewers' comments

Manuscript No.: acp-2018-701

Title: Quantification and evaluation of atmospheric pollutant emissions from open biomass burning with multiple methods: A case study for Yangtze River Delta region, China

Authors: Yang Yang, Yu Zhao

We thank very much for the valuable comments and suggestions from the two reviewers, which help us improve our manuscript. The comments were carefully considered and revisions have been made in response to suggestions. Following is our point-by-point responses to the comments and corresponding revisions.

Reviewer #1

1. General comments: This manuscript presents a very comprehensive study of historical trend of OBB emissions in YRD. I am very impressed by the large amounts of work done in this study. The presentation is also of high quality, and the structure is well organized. The constraining method is a little bit weak, but makes the story complete. I would suggest the authors improve the constraining method in future studies. The authors have acknowledged the weakness, which is great. I only have very minor comment for improvements. For constraining method, the correction is based on the comparisons of PM10, and the correction factor was applied to all other species. The authors should acknowledge this limitation in the method section.

Response and revisions:

We appreciate the reviewer's positive remarks on our manuscript. We thank the reviewer's suggestion and will improve the constraining method in future studies

from following aspects. The method can be improved incorporating the observed ambient concentrations of multiple pollutants (e.g., PM₁₀, PM_{2.5}, OC and EC) if those concentrations with sufficient temporal and spatial resolution get available. Improvement on the results of constraining method can be expected if more reliable emission factors of biomass burning and improved and the emissions of other sources are obtained and applied in the study. For constraining method, the correction of activity level was based on the comparison between simulated and observed PM₁₀ concentrations, and the emissions of other species were then revised according to the changed activity level. In this method, the emission estimation of other species depends largely on the reliability of emission factors for PM₁₀ and those species. Large uncertainty may exist due to lack of sufficient domestic measurements. We take the reviewer's suggestion and acknowledge this limitation in the method section. **Corresponding revision was shown in lines 258-264 of Page 9 in the revised manuscript.**

Reviewer #2

1. This manuscript estimates the air pollutant emissions from open biomass burning(OBB) in Yangtze River Delta for 2005-2015 using traditional bottom-up, fire radiative power (FRP)-based, and constraining approaches, and analyzed the differences between those methods and their underlying reasons. The manuscript is generally well written. However, there are still some issues in the manuscript which authors shall pay attention to. So the paper cannot be accepted for publication before authors address the following comments.

Response and revisions:

We appreciate the reviewer's crucial and important comments. In general, the presentation of the work has been improved, based on specific comments/suggestion from the reviewer. Same emission factors as bottom-up method were applied to estimate the OBB emissions for 2010 based on FRP-based method, and the results

were compared with those based on bottom-up method. Both PM_{2.5} and PM₁₀ concentrations were used to evaluate the model performance and to analyze the contribution of OBB in June 7-13, 2014. The benchmarks of the evaluation for model performance and meteorological parameters were added in Table 2 and Table S6 in the supplement. We also take the reviewer's suggestion and provide the monthly variations of fire occurrence for other years in Figure S3 in the supplement. Details follow.

2. As shown in Table S1 and Table S4, the authors use different emission factors for OBB in bottom-up method and FRP-based method. I suggest same emission factors shall be used for both methods. This is why that for most air pollutants, emissions estimated by bottom-up method is higher than that by FRP-based but the emissions of NMVOC and NH₃ from bottom-up method is much lower than that by FRP-based method.

Response and revisions:

We thank the reviewer's comment. In the bottom-up method, the masses of crop residues burned in the field (CRBF) for different crop species could be obtained, therefore the emission factors for different crop types were usually used. However, the masses of CRBF for different crop species in FRP-based method could not be obtained, and the emission factors based on burned area or fire radiative power (BA or FRP method) by other researchers (van der Werf et al., 2010, Kaiser et al., 2012; Liu et al., 2015; Randerson et al., 2018) were applied, ignoring the difference between crop types. In order to know the differences between the OBB emissions based on FRP-based and bottom-up methods with same emission factors, we followed the reviewer's comment and made an extra case: the emission factors applied in the bottom-up method were weighted with the masses of various crop types and used to estimate the OBB emissions for 2010 with the FRP-based method. The estimated OBB emissions (FRP-based (WSE)) were compared with the emissions based on

bottom-up method as shown in Table 3. The OBB emissions for all species in FRP-based (WSE) were smaller than those derived by bottom-up method. The differences in OBB emissions between bottom-up and FRP-based (WSE) method were larger than 50% of those between the bottom-up and the original FRP-based method with different emission factors for most species. It indicated that the discrepancy in activity level contributed the most to the difference in OBB emissions between bottom-up and FRP-based method. **Corresponding revision was shown in lines 200-205 of Page 7 and lines 553-559 of Page 18 in the revised manuscript.**

3. The spatial resolutions of the two domains were set at 27 and 9 km respectively. 9km is kind of coarse resolution. How does this spatial resolution affect the CMAQ modeling results? Will you get a better model performance if you use a 3km resolution?

Response and revisions:

We thank the reviewer's comment. The model performance largely depends on the reliability of emission inventories. The emissions of other sources in this study were obtained from the downscaled the Multi resolution Emission Inventory for China (MEIC) with an original spatial resolution of $0.25^{\circ} \times 0.25^{\circ}$. The model performance with a finer resolution might not necessarily be better since the emissions were probably not distributed in the correct grids in finer resolution with a simple spatial interpolation (Zheng et al., 2017). Improvement on emission inventory with the underlying data carefully compiled and analyzed is important to achieve better model performance with high-resolution chemistry transport modeling. Our previous study by Zhou et al. (2017) evaluated the downscaled MEIC and improved local emission inventory with CMAQ modeling at a 3 km resolution in southern Jiangsu of Yangtze River Delta (YRD), and found the model performance was better for the latter inventory. Once the emission inventory of all the anthropogenic sources get improved for the whole YRD region, therefore, a better model performance with high-resolution modeling (e.g., 3km) can be expected.

4. Considering that the PM emissions from OBB are mainly $PM_{2.5}$, and the ambient PM_{10} is more affected by the local road dust emissions, it is not appropriate to only use PM_{10} concentration to evaluate the model performance and analyze the contribution of OBB. I think authors shall use both PM_{10} , $PM_{2.5}$, CO, NO_2 , SO_2 , OC, EC to do the model evaluation. At least $PM_{2.5}$ shall be included considering that most Chinese cities release $PM_{2.5}$ hourly concentrations since 2013. Although authors give a couple of figures in SI, this is not enough. Specifically, the correction based on the comparisons of PM_{10} cannot be used for all other species.

Response and revisions:

We thank the reviewer's comment. We agree with the reviewer that observation of more relevant species should ideally be included in the constraining method and evaluation of OBB emissions. However, the most and the second most fire counts were found for YRD region in 2012 and 2010 from 2005 to 2015, while the concentrations of $PM_{2.5}$, CO, NO_2 , and SO_2 were unavailable before 2013. The largest daily mass ratio of $PM_{2.5}$ to PM_{10} could reach 91.3% in Nanjing during the OBB event of 2012 and 77.2% in Lianyungang during the event of 2014. The contribution of OBB to PM_{10} estimated in this study was 37% in YRD and 55% in Anhui province during OBB period in June 2012. The OBB could thus be identified as an important source of PM_{10} during the OBB event periods as well. Therefore, we used PM_{10} concentration to evaluate the model performance and analyze the contribution of OBB in 2010 and 2012. Compared to $PM_{2.5}$ and PM_{10} , OBB was not a major source of NO_2 and SO_2 , and the OC and EC concentrations were still unavailable at present as they were not considered as regulated pollutants in China. In this case, we followed the reviewer's suggestion and applied both $PM_{2.5}$ and PM_{10} concentrations to evaluate the model performance and analyze the contribution of OBB in June 7-13, 2014. Similar to 2010 and 2012, the NMBs and NMEs between observed and simulated particle concentrations with constrained OBB emissions were smaller than most of those without OBB emissions or with OBB emissions based on FRP-based. **Corresponding**

revision was shown in lines 459-475 of Page 15 and 490-498 of Page 16 in the revised manuscript. The average contributions of OBB to PM_{2.5} and PM₁₀ during June 7-13, 2014 were estimated at 29% and 23% for 22 cities in YRD. It again suggested that the OBB was an important source of both PM_{2.5} and PM₁₀ during OBB event. **Corresponding revision was shown in lines 587-593 and lines 605-607 of Page 19 in the revised manuscript.**

We also admitted the limitation of constrained method, as our response to Question 1 of Reviewer 1. We agree with the reviewer that the concentrations of PM_{2.5} or OC were more suitable for constraining OBB emissions. However, the data were unavailable before 2013, particularly for 2010 and 2012 with the most and the second most fire counts detected by satellite. As OBB was an important source of PM₁₀ as well, we had to apply PM₁₀ concentrations to constrain the OBB emissions. The activity level was constrained based on the comparisons between simulated and observed PM₁₀ concentrations, and the OBB emissions of other species were revised according to the changed activity level. The reliability of emissions for other species depended largely on the accuracy of emission factors for PM₁₀ and those species. Uncertainties would be introduced to the emission estimation, resulting from lack of sufficient and qualified domestic field tests on OBB emission factors. We admit this limitation in the method section, and improvement can be expected with more measurements on concentrations of multiple pollutants and local emission factors available in the future. **Corresponding revision was shown in lines 258-264 of Page 9 in the revised manuscript.**

5. The model performance statistics for meteorological parameters shown in Table S6 and that for PM10 concentrations as shown in Table 2 shall include the benchmark of the evaluation.

Response and revisions:

We thank the reviewer's comment. The benchmarks of the evaluation for meteorological parameters from Emery et al. (2001) and Jiménez et al. (2006) were

added in Table S6. The meteorological parameters of this study were basically in compliance with benchmarks. **Corresponding revision was shown in lines 312-317 of Page 11 in the revised manuscript.**

As many factors would influence the model performance of chemistry transport model, no uniform benchmark was obtained for different regions. We selected the results in US (Zhang et al., 2006) as the benchmark for PM_{2.5} and PM₁₀ concentrations, as added in Table 2. As can be found in the table, the NMBs and NMEs for most case with the constrained OBB emissions were close to those by Zhang et al. (2006). The NMEs for hourly PM_{2.5} and PM₁₀ were slightly larger. Given the larger uncertainty in emission inventory of anthropogenic sources for China and the uncertainty in spatial and temporal distribution of OBB emissions due to satellite detection limit, we believe the model performance with the constrained OBB emissions was improved and acceptable. **Corresponding revision was shown in lines 490-498 of Page 16 in the revised manuscript.**

6. For OBB, temporal allocation is very important. It is good to see the monthly variations of fire occurrence in Figure 1. However, the authors only give information for year 2010 and 2012, I wonder if the authors can provide such information for other years.

Response and revisions:

We thank the reviewer's suggestion and provide the information for other years (2005-2015) in Figure S3 in supplement.

7. Figure 2 shall give the name of each city in the YRD. Otherwise it is difficult for readers to understand when author talk about Lianyungang, Fuyang, Shanghai, Suzhou, Wuxi, Changzhou, etc.

Response and revisions:

We thank the reviewer's suggestion and provide the name of each city in the YRD in Figure 2.

8. The color in Figure 4 is very difficult to read.

Response and revisions:

We thank the reviewer's reminder. We applied thicker lines and changed the colors to make the figure easier to read.

References

- Emery, C., Tai, E., and Yarwood, G.: Enhanced meteorological modeling and performance evaluation for two Texas episodes, Report to the Texas Natural Resources Conservation Commission, prepared by ENVIRON, International Corp, Novato, CA, 2001.
- Kaiser, J. W., Heil, A., Andreae, M. O., Benedetti, A., Chubarova, N., Jones, L., Morcrette, J. J., Razinger, M., Schultz, M. G., Suttie, M., and van der Werf, G. R.: Biomass burning emissions estimated with a global fire assimilation system based on observed fire radiative power, *Biogeosciences*, 9, 527–554, doi: 10.5194/bg-9-527-2012, 2012.
- Liu, M. X., Song, Y., Yao H., Kang, Y. N., Li, M. M., Huang, X., and Hu, M.: Estimating emissions from agricultural fires in the North China Plain based on MODIS fire radiative power, *Atmos. Environ.*, 112, 326–334, 2015.
- Jiménez, P., Jorba, O., Parra R. and Baldasano J. M.: Evaluation of MM5-EMICAT2000-CMAQ performance and sensitivity in complex terrain: High-resolution application to the northeastern Iberian Peninsula, *Atmos. Environ.*, 40, 5056-5072, doi:10.1016/j.atmosenv.2005.12.060, 2006.
- Randerson, J. T., van der Werf, G. R., Giglio, L., Collatz, G. J., and Kasibhatla, P. S.: Global Fire Emissions Database, Version 4.1 (GFEDv4). ORNL DAAC, Oak Ridge, Tennessee, USA. <https://doi.org/10.3334/ORNLDAAC/1293>, 2018.
- van der Werf, G. R., Randerson, J. T., Giglio, L., Collatz, G. J., Mu, M., Kasibhatla, P. S., Morton, D. C., DeFries, R. S., Jin, Y., and van Leeuwen, T. T.: Global fire emissions and the contribution of deforestation, savanna, forest, agricultural, and peat fires (1997-2009), *Atmos. Chem. Phys.*, 10, 11707-11735, doi: 10.5194/acp-10-11707-2010, 2010.
- Zheng, B., Zhang, Q., Tong, D, Chen, C. C., Hong, C. P., Li, M., Geng, G. N., Lei, Y., Huo, H. and He, K. B.: Resolution dependence of uncertainties in gridded emission inventories: a case study in Hebei, China, *Atmos. Chem. Phys.*, 17, 921–933, doi:10.5194/acp-17-921-2017, 2017.
- Zhang, Y., Liu, P., Pun, B., and Seigneur, C.: A comprehensive performance evaluation of MM5-CMAQ for the Summer 1999 Southern Oxidants Study episode-Part I: Evaluation protocols, databases, and meteorological predictions, *Atmos. Environ.*, 40, 4825–4838, 2006.
- Zhou, Y. D., Zhao Y., Mao P., Zhang Q, Zhang J., Qiu, L. P., and Yang, Y.: Development of a high-resolution emission inventory and its evaluation and application through air quality modeling for Jiangsu Province, China, *Atmos. Chem. Phys.*, 17, 211–233, 2017.

1
2
3
4
5
6
7
8
9
10
11
12
13
14
15
16
17

Quantification and evaluation of atmospheric pollutant emissions from open biomass burning with multiple methods: A case study for Yangtze River Delta region, China

Yang Yang¹ and Yu Zhao^{1,2*}

1. State Key Laboratory of Pollution Control & Resource Reuse and School of the Environment, Nanjing University, 163 Xianlin Ave., Nanjing, Jiangsu 210023, China
2. Jiangsu Collaborative Innovation Center of Atmospheric Environment and Equipment Technology (CICAEET), Nanjing University of Information Science & Technology, Jiangsu 210044, China

*Corresponding author: Yu Zhao
Phone: 86-25-89680650; email: yuzhao@nju.edu.cn

Abstract

18
19 Air pollutant emissions from open biomass burning (OBB) in Yangtze River
20 Delta (YRD) were estimated for 2005-2015 using three (traditional bottom-up, fire
21 radiative power (FRP)-based, and constraining) approaches, and the differences
22 between those methods and their sources were analyzed. The species included PM₁₀,
23 PM_{2.5}, organic carbon (OC), ~~black~~-elemental carbon (BCEC), CH₄, non-methane
24 volatile organic compounds (NMVOCs), CO, CO₂, NO_x, SO₂ and NH₃. The
25 inter-annual trends in emissions with FRP-based and constraining methods were
26 similar with the fire counts in 2005-2012, while that with traditional method was not.
27 For most years, emissions of all species estimated with constraining method were
28 smaller than those with traditional method except for NMVOCs, while they were
29 larger than those with FRP-based except for EC, CH₄ and NH₃. Such discrepancies
30 result mainly from different masses of crop residues burned in the field (CRBF)
31 estimated in the three methods. Chemistry transport modeling (CTM) was applied
32 using the three OBB inventories. The simulated PM₁₀ concentrations with constrained
33 emissions were closest to available observations, implying constraining method
34 provided the best emission estimates. CO emissions in the three methods were
35 compared with other studies. Similar temporal variations were found for the
36 constrained emissions, FRP-based emissions, GFASv1.0 and GFEDv4.1s, with the
37 largest and the lowest emissions estimated for 2012 and 2006, respectively. The
38 temporal variations of the emissions based on traditional method, GFEDv3.0 and Xia
39 et al. (2016) were different with them. The constrained CO emissions in this study
40 were commonly smaller than those based on traditional bottom-up method and larger
41 than those based on burned area or FRP in other studies. In particular, the constrained
42 emissions were close to GFEDv4.1s that contained emissions from small fires. The
43 contributions of OBB to two particulate pollution events in 2010 and 2012 were
44 analyzed with brute-force method. Attributed to varied OBB emissions and
45 meteorology, the average contribution of OBB to PM₁₀ concentrations in June 8-14
46 2012 was estimated at 37.6% (56.7 μg/m³), larger than that in June 17-24, 2010 at
47 21.8 % (24.0 μg/m³). Influences of diurnal curves of OBB emissions and meteorology
48 on air pollution caused by OBB were evaluated by designing simulation scenarios,
49 and the results suggested that air pollution caused by OBB would become heavier if
50 the meteorological conditions were unfavorable, and that more attention should be

51 paid to the OBB control at night. Quantified with Monte-Carlo simulation, the
52 uncertainty of traditional bottom-up inventory was smaller than that of FRP-based one.
53 The percentages of CRBF and emission factors were the main source of uncertainty
54 for the two approaches, respectively. Further improvement on CTM for OBB events
55 would help better constraining OBB emissions.

56

57

1. Introduction

58 Open biomass burning (OBB) is an important source of atmospheric particulate
59 matter (PM) and trace gases including methane (CH₄), non-methane volatile organic
60 compounds (NMVOCs), carbon monoxide (CO), carbon dioxide (CO₂), oxides of
61 nitrogen (NO_x), sulfur dioxide (SO₂), and ammonia (NH₃) (Andreae and Merlet, 2001;
62 van der Werf et al., 2010; Wiedinmyer et al., 2011; Kaiser et al., 2012; Giglio et al.,
63 2013, Qiu et al., 2016; Zhou et al., 2017a). As it has significant impacts on air quality
64 and climate (Crutzen and Andreae, 1990; Cheng et al., 2014; Hodzic and Duvel, 2018),
65 it is important to understand the amount, temporal variation and spatial pattern of
66 OBB emissions.

67 Various methods have been used to estimate OBB emissions, including
68 traditional bottom-up method that relied on surveyed amount of biomass burning
69 (traditional bottom-up method), the method based on burned area or fire radiative
70 power (BA or FRP method), and emission constraining with chemistry transport
71 model (CTM) and observation (constraining method). In the traditional bottom-up
72 method that was most frequently used, emissions were calculated as a product of crop
73 production level, the ratio of straw to grain, percentage of dry matter burned in fields,
74 combustion efficiency, and emission factor (Streets et al., 2003; Cao et al., 2007;
75 Wang and Zhang, 2008; Zhao et al., 2012; Xia et al., 2016, Zhou et al., 2017a). The
76 BA or FRP method was developed along with progress of satellite observation
77 technology. BA was detected through remote sensing, and used in OBB emission
78 calculation combined with ground biomass density burned in fields, combustion
79 efficiency and emission factor. As burned area of each agricultural fire was usually
80 small and difficult to be detected, this method could seriously underestimate the
81 emissions (van der Werf et al., 2010; Liu et al., 2015). In FRP-based method, fire
82 radiative energy (FRE) was calculated with FRP at over pass time of satellite and the
83 diurnal cycle of FRP. The mass of crop residues burned in the field (CRBF) were then

84 obtained based on combustion conversion ratio and FRE, and emissions were
85 calculated as a product of the mass of CRBF and emission factor (Kaiser et al., 2012;
86 Liu et al., 2015). In the constraining method, observed concentrations of atmospheric
87 compositions were used to constrain OBB emissions with CTM (Hooghiemstra et al.,
88 2012; Krol et al., 2013; Konovalov et al., 2014). The spatial and temporal
89 distributions of OBB emissions were derived from information of fire points from
90 satellite observation. Although varied methods and data sources might lead to
91 discrepancies in OBB emission estimation, those discrepancies and underlying
92 reasons have seldom been thoroughly analyzed in previous studies. Moreover, few
93 studies applied CTM to evaluate emissions obtained from different methods, thus the
94 uncertainty and reliability in OBB emission estimates remained unclear.

95 Due to growth of economy and farmers' income, a large number of crop straws
96 were discharged and burned in field, and OBB (which refers to crop straws burned in
97 fields in this paper) became an important source of air pollutants in China (Streets et
98 al., 2003; Shi and Yamaguchi 2014; Qiu et al., 2016; Zhou et al., 2017a). It brings
99 additional pressure to the country, which is suffering poor air quality (Richter et al.,
100 2005; van Donkelaar et al., 2010; Xing et al., 2015; Guo et al., 2017) and making
101 efforts to reduce pollution (Xia et al., 2016; Zheng et al., 2017). Located in the eastern
102 China, Yangtze River Delta (YRD) including the city of Shanghai and the provinces
103 of Anhui, Jiangsu and Zhejiang is one of China's most developed and heavy-polluted
104 regions (Ran et al., 2009; Xiao et al., 2011; Cheng et al., 2013, Guo et al., 2017).
105 Besides intensive industry and fossil fuel combustion, YRD is also an important area
106 of agriculture production, and frequent OBB events aggravated air pollution in the
107 region (Cheng et al., 2014).

108 In this study, we chose YRD to develop and evaluate high resolution emission
109 inventories of OBB with different methods. Firstly, we established YRD's OBB
110 emission inventories for 2005-2012 using the traditional bottom-up method (the
111 percentages of CRBF for 2013-2015 were currently unavailable), and inventories for
112 2005-2015 using FRP-based and constraining methods. The three inventories were
113 then compared with each other and other available studies, in order to discover the
114 differences and their origins. Meanwhile, the three inventories were evaluated using
115 Models-3 Community Multi-scale Air Quality (CMAQ) system and available ground
116 observations. Contributions of OBB to particulate pollution during ~~two~~three typical
117 OBB events in 2010 ~~and~~ 2012 and 2014 were evaluated through brute-force method.

118 Influences of meteorology and diurnal curves of OBB emissions on air pollution
119 caused by OBB were also analyzed by designing simulation scenarios. Finally,
120 uncertainties of the three OBB inventories were analyzed and quantified with
121 Monte-Carlo simulation.

122

123

2. Data and methods

2.1 Traditional bottom-up method

124 Annual OBB emissions in YRD were calculated by city from 2005 to 2012 using
125 the traditional bottom-up method with following equations:
126

$$127 \quad E_{(i,y),j} = \sum_k (M_{(i,y),k} \times EF_{j,k}) \quad (1)$$

$$128 \quad M_{(i,y),k} = P_{(i,y),k} \times R_k \times F_{(i,y)} \times CE_k \quad (2)$$

129 where i and y indicate city and year (2005-2012), respectively; j and k represent
130 species and crop type, respectively; E is the emissions, metric ton (t); M is the mass of
131 CRBF, Gg; EF is the emission factor, g/kg; P is the crop production, Gg; R is the ratio
132 of grain to straw (dry matter); F is the percentage of CRBF; and CE is the combustion
133 efficiency.

134 As summarized in Table S1 in the supplement, emission factors were obtained
135 based on a comprehensive literature review, and those developed in China were
136 selected preferentially. The mean value was used if various emission factors could be
137 obtained. When the emission factors for one crop straw were not obtained, the mean
138 value of the others was used instead. Annual production of crops at city level was
139 taken from statistical yearbooks (NBS, 2013). The ratios of straw to grain for different
140 crops were obtained from Bi (2010) and Zhang et al. (2008), and the combustion
141 efficiencies for different crop were obtained from Wang et al. (2013), as provided in
142 Table S2 in the supplement. Without officially reported data, the percentages of CRBF
143 were estimated to be half of the percentages of unused crop residues, following Su et
144 al. (2012). In Jiangsu, the percentages of unused crop residues were officially reported
145 for 2008, 2011 and 2012, while data for other years were unavailable. In this work,
146 therefore, the percentages of CRBF were assumed to be constant before 2008 and to
147 decrease by same rate (-15.2%) from 2008 to 2011, since a provincial plan was made
148 in 2009 to increase the utilization of straw (JPDRC and SMAC, 2009). Similarly, the
149 percentages of CRBF for Shanghai were assumed to be constant before 2008 and to

150 decrease by same rate (-16.8%) from 2008 to 2012. Without any official plans
 151 released, in contrast, constant percentages of CRBF were assumed for Zhejiang and
 152 Anhui before 2011, and that for 2012 was taken from NDRC (2014). We applied
 153 uniform percentages of CRBF for cities within a province attributed to lack of detailed
 154 information at city level, as summarized in Table S3 in the supplement. OBB
 155 emissions after 2012 were not calculated with the traditional bottom-up method,
 156 attributed to lack of information on percentages of CRBF and unused crop residues
 157 for corresponding years.

158 2.2 FRP-based method

159 Similar to traditional bottom-up method, OBB emissions of FRP-based method
 160 were calculated by multiplying the mass of CRBF and emission factors of various
 161 pollutants, but mass of CRBF were derived from FRP instead of government-reported
 162 data. As the burned crop types could not be identified with FRP, uniform emission
 163 factors were applied for different crop types (Randerson et al., 2015; Liu et al.,
 164 2016; Qiu et al., 2016), as provided in Table S4 in the supplement.

165 The mass of CRBF was calculated with the following equation:

$$166 \quad M = FRE \times CR \quad (3)$$

167 where M represents the mass of CRBF, kg; CR represents the combustion conversion
 168 ratio from energy to mass (kg/MJ); and FRE represents the total released radiative
 169 energy in an active fire pixel obtained from satellite observation (MJ). We used a
 170 combustion ratio (CR) of 0.41 ± 0.04 (kg/MJ) based on the results of Wooster et al.
 171 (2005) in the field and Freeborn et al. (2008) in the laboratory. Diurnal cycle of FRP
 172 from crop burning was assumed to follow a Gaussian distribution. Following Vermote
 173 et al. (2009) and Liu et al. (2015), FRE was calculated using a modified Gaussian
 174 function as below:

$$175 \quad FRE = \int FRP = \int_0^{24} FRP_{peak} \left(b + e^{-\frac{(t-h)^2}{2\sigma^2}} \right) dt \quad (4)$$

$$176 \quad FRE_{peak} = \frac{FRP_t}{\left[b + e^{-\frac{(t-h)^2}{2\sigma^2}} \right]} \quad (5)$$

177 where FRP_{peak} is the peak fire radiative power in the fire diurnal cycle; t is the
 178 overpass time of satellite; and b , σ , and h represent the background level of the diurnal
 179 cycle, the width of fire diurnal curve, and the peak hour (local time, LT), respectively.

180 FRP data were taken from MODIS Global Monthly Fire Location Product
181 (MCD14ML) which provides data from both the Terra and Aqua satellites (Davies et
182 al., 2009). The active fire data in MCD14ML were derived from Terra with overpass
183 times at approximately 10:30 AM and 10:30 PM LT and Aqua satellite with overpass
184 times at 1:30 AM and 1:30 PM LT. The fire products provided the geographic
185 coordinates of fire pixels (also known as fire points), overpass times, satellites and
186 their FRP values. The land cover dataset (GlobCover2009) was used to define
187 croplands (European Space Agency and Université Catholique de Louvain, 2011).

188 Parameters b , σ , and h from 2005 to 2015 were calculated using the inter-annual
189 Terra to Aqua (T/A) FRP ratios provided in Table S5 in the supplement:

$$190 \quad b = 0.86r^2 - 0.52r + 0.08 \quad (6)$$

$$191 \quad \sigma = 3.89r + 1.03 \quad (7)$$

$$192 \quad h = -1.23r + 14.57 + \varepsilon \quad (8)$$

193 where r represents the average T/A FRP ratio. Following Liu et al. (2015), we added a
194 parameter ε (4h) to modify FRP_{peak} hour (h) of the diurnal curve, and the modified
195 FRP diurnal curves could better represent observed FRP temporal variability than the
196 original, as shown in Figure S1 in the supplement. As a result, FRE was calculated to
197 range from 1.49×10^6 MJ in 2009 to 1.95×10^6 MJ in 2005, with a mean value of
198 1.74×10^6 MJ for YRD region (Table S5).

199 To further understand the sources of discrepancies between bottom-up and
200 FRP-based methods, the emission factors applied in the bottom-up method were
201 weighted with the masses of various crop types and used to estimate the OBB
202 emissions for 2010 with the FRP-based method. The estimated OBB emissions
203 (FRP-based (WSE)) were compared with the emissions based on bottom-up method in
204 section 3.3.

205 **2.3 Constraining method**

206 CTM and observation of ground particle matter (PM) concentrations were
207 applied in constraining OBB emissions given the potentially big contribution of OBB
208 to particle pollution for harvest seasons (Fu et al., 2013; Cheng et al., 2014; Li et al.,
209 2014). To characterize the non-linearity between emissions and concentrations, an
210 initial inventory including OBB and other sources was applied in CTM, and the
211 response of PM concentrations to emissions was calculated by changing OBB
212

214 emissions by a certain fraction (5% in this study) in the model. We defined a response
 215 coefficient as the ratio of relative change in PM concentrations to that in OBB
 216 emissions. Simulated PM concentrations were then compared with available
 217 observation, and the mass of CRBF and OBB emissions of all species were corrected
 218 combining the obtained response coefficient and the discrepancy between observed
 219 and simulated PM concentrations. The corrected emissions were further applied in
 220 CTM and the process (including recalculation of response coefficient) repeated until
 221 the discrepancies between observation and simulation was small enough (the value of
 222 I in equation (9) is less than 0.1% in this study). To limit the potential uncertainty in
 223 emissions from other sources, the differences between simulated and observed PM
 224 concentrations for non-OBB event period were included in the analysis:

$$225 \quad I = \left| \frac{\sum_{x,i} S_{x,i} - \sum_{x,i} Q_{x,i} \times N_i}{\sum_{x,i} O_{x,i}} - 1 \right| \quad (9)$$

226 where x and i stand for the time (time interval of simulation is hour) and city,
 227 respectively; O is the observed PM concentration; S and Q are the simulated PM
 228 concentration with and without OBB emissions, respectively; and N is the normalized
 229 mean bias (NMB) for non-OBB event period.

230 As primary particles emitted from OBB are almost fine ones, ambient $PM_{2.5}$
 231 concentrations were commonly observed to account for large fractions of PM_{10} during
 232 the OBB event. Figure S2 shows the observed concentrations of $PM_{2.5}$ and PM_{10} at
 233 Caochangmen station in Nanjing (the capital of Jiangsu) in June 2012, and the
 234 average mass ratio of $PM_{2.5}$ to PM_{10} reached 79% during the OBB event in June 8-14,
 235 2012. The ratios might be even higher in northern YRD where most fire points were
 236 detected. As ground $PM_{2.5}$ concentrations were unavailable in most cities of northern
 237 YRD before 2013, we expected that PM_{10} was an appropriate indicator for OBB
 238 pollution, and observed PM_{10} concentrations were used to constrain OBB emissions
 239 instead in this study. The daily mean PM_{10} concentrations of all cities were derived
 240 from the officially reported Air Pollution Index (API) by China National
 241 Environmental Monitoring Center (<http://www.cnemc.cn/>). The conversion from API
 242 scores to PM_{10} concentrations is discussed in the Supplement.

243 | Figure 1 illustrated the ~~monthly variations of fire occurrences in 2010 and 2012~~
 244 | (~~panels a1 and a2, respectively~~), spatial patterns of fire points (panels ~~b1-a1~~ and ~~b2-a2~~)

245 in June 2010 and 2012, city-level PM₁₀ concentrations in YRD region in June 2010
246 and 2012 (panels [e1-b1](#) and [e2-b2](#)), and temporal variations of daily fire occurrences in
247 June 2010 and 2012 (panels [d1-c1](#) and [d2-c2](#)). From 2005 to 2012, most OBB
248 activities were found in June 2010 and 2012 and northern YRD was the region with
249 the intensive fire counts. Accordingly PM₁₀ concentrations in northern YRD cities
250 were higher than those in more developed and industrialized cities in the eastern YRD
251 (e.g., Shanghai, Suzhou, Wuxi, and Changzhou), because emissions of OBB
252 overwhelmed those from other sources (Li et al., 2014; Huang et al., 2016). Therefore
253 we constrained OBB emissions with observed PM₁₀ concentrations in northern YRD
254 cities including Xuzhou, Lianyungang, Fuyang, Bengbu, Huainan, Hefei, Chuzhou
255 and Bozhou. Suggested by the monthly and daily distribution of fire counts (Figures
256 [1a-S3](#) and [1d1c](#)), two strong OBB events were defined for June 17-24, 2010 and June
257 8-14, 2012, and other days in June of 2010 and 2012 were defined as non-OBB event
258 period. For other years, OBB emissions were first scaled from the constrained
259 emissions in 2010 and 2012 with the ratios of FRE for corresponding year to that for
260 2010 and 2012 respectively, and then calculated as average of the two. Remarkably,
261 the correction of activity level was based on the comparisons of simulated and
262 observed PM₁₀ concentrations in constraining method, and then the emissions of other
263 species were changed revised based on according to the corrected changed activity
264 level. The reliability of emissions estimation for other species based on this method
265 thus depended was largely depend on the accuracy reliability of emission factors for
266 PM₁₀ and those species. Uncertainty It brought would be introduced t some
267 uncertainties to the emissions of those speciee method,s due attributed to the lack of
268 sufficient and qualified uncertainties domestic measurements on of emission factors.
269 Moreover, the uncertainty of constrained OBB emission from other reasons was
270 analyzed in section 3.5.

271 Traditional bottom-up method was used to calculate the initial emission input for
272 all species (NMVOCs emission factor was taken from FRP-based method instead as
273 those in bottom-up method (Li et al., 2007) did not contain oxygenated VOCs). In
274 contrast to application of uniform percentage of CRBF within one province, however,
275 percentage of CRBF for each city was calculated based on that in whole YRD and the
276 fraction of FRP in the city to total YRD FRP, to make the spatial distribution of OBB
277 emissions consistent with that of FRP all over YRD region:

$$F_{(i,y)} = \frac{FRP_{(i,y)}}{FRP_{(YRD,y)}} \times \frac{\sum_k P_{(YRD,y),k}}{\sum_k P_{(i,y),k}} \times F_{(YRD,y)} \quad (10)$$

where i and k represent city and crop type, respectively; y indicates the year (2010 and 2012); F , P , and FRP are the percentage of CRBF, crop production, and fire radiative power, respectively. The initial percentage of CRBF for total YRD ($F_{(YRD,y)}$ in eq (10)) was expected to have limited impact on the result and it was set at 10%, smaller than those in previous studies (Streets et al., 2003; Cao et al., 2007; Wang and Zhang, 2008; Zhao et al., 2012; Xia et al., 2016, Zhou et al., 2017a).

2.4 Temporal and spatial distributions

The spatial and temporal patterns of OBB emissions in the three inventories were determined according to the FRP of agricultural fire points. The emissions of m -th grid in region u on n -th day in year y were calculated using equation (11):

$$E_{(m,n),j} = \frac{FRP_{(m,n)}}{FRP_{(u,y)}} \times E_{(u,y),j} \quad (11)$$

where $FRP_{(m,n)}$ is the FRP of m -th grid on n -th day; $FRP_{(u,y)}$ and $E_{(u,y),j}$ are the total FRP and OBB emissions of species j for region u in year y , respectively. The region u indicates city for FRP-based and constraining method, while it indicates province for traditional bottom-up method since uniform percentages of CRBF was applied within the same province in the method.

2.5 Configuration of air quality modeling

The Models-3 Community Multi-scale Air Quality (CMAQ) version 4.7.1 was applied to constrain OBB emissions and to evaluate OBB inventories with different methods. As shown in Figure 2, one-way nested domain modeling was conducted, and the spatial resolutions of the two domains were set at 27 and 9 km respectively in Lambert Conformal Conic projection, centered at (110°E, 34°N) with two true latitudes 25 and 40° N. The mother domain (D1, 180×130 cells) covered most parts of China, Japan, North and South Korea, while the second domain (D2, 118×97 cells) covered the whole YRD region. OBB inventories developed in this work were applied in D2. Emissions from other anthropogenic sources in D1 and D2 were obtained from the downscaled the Multi resolution Emission Inventory for China (MEIC, <http://www.meicmodel.org/>) with an original spatial resolution of 0.25°×0.25°. Population density was applied to relocate MEIC to each modeling domain. Biogenic

308 emission inventory was from the Model Emissions of Gases and Aerosols from
309 Nature developed under the Monitoring Atmospheric Composition and Climate
310 project (MEGAN MACC, Sindelarova et al., 2014), and the emission inventories of
311 Cl, HCl and lightning NO_x were from the Global Emissions Initiative (GEIA, Price et
312 al., 1997). Meteorological fields were provided by the Weather Research and
313 Forecasting Model (WRF) version 3.4, and the carbon bond gas-phase mechanism
314 (CB05) and AERO5 aerosol module were adopted. Other details on model
315 configuration and parameters were given in Zhou et al. (2017b).

316 Meteorological parameters of WRF model were compared with the observation
317 dataset of US National Climate Data Center (NCDC), as summarized in Table S6 in
318 the Supplement. For June 2010, the average biases between the two datasets were
319 0.06 m/s for wind speed, 9.84 degree for wind direction, 0.64 K for temperature and
320 2.99% for relative humidity.~~For June 2012, the average biases between the two~~
321 ~~datasets were 0.01 m/s for wind speed, -7 degree for wind direction, 0.91 K for~~
322 ~~temperature and 3.1% for relative humidity. The analogue numbers were 0.01 and~~
323 ~~0.67 m/s, 7 and 18.22 degree, 0.91 and 0.43 K and 3.1 and 0.07% respectively for~~
324 ~~June 2012 and 2014, respectively.~~~~The analogue numbers were 0.06 m/s, 9.84 degree,~~
325 ~~0.64 K and 2.99% respectively for June 2010. The meteorological parameters of this~~
326 ~~study were basically in compliance with -conformity to- the benchmarks derived from~~
327 ~~Emery et al. (2001) and Jiménez et al. (2006).~~ Simulated daily PM₁₀ concentrations
328 were compared with observation for non-OBB event period in June 2010 and 2012 in
329 Table S7 in the supplement. The average of normalized mean biases (NMB) and
330 normalized mean errors (NME) were -19.92% and 38.9% for 17 YRD cities in June
331 2010, and -2220.98% and 33.9% for 22 cities in June 2012, respectively. Simulated
332 daily and hourly PM₁₀ and PM_{2.5} concentrations were compared with the observation
333 for non-OBB event period in June 2014 in Table S8 in the supplement. The hourly
334 NMB of PM_{2.5} and PM₁₀ were -29.9% and -39.8%, and the hourly NME of PM_{2.5} and
335 PM₁₀ were 49.8% and 54.7%. The model performance was similar with that derived
336 by Zhang et al. (2006) in US in general. As shown in Figure ~~S3-S4~~ in the supplement,
337 moreover, simulated hourly PM₁₀ and PM_{2.5} concentrations were in good agreement
338 with observations at four air quality monitoring sites in YRD during non-OBB event
339 period in June 2012. The comparison thus implied the reliability of emission
340 inventory of anthropogenic origin used in this work, while underestimation might
341 occur indicated by the negative NMB.

342

343

3. Results and discussions

3.1 OBB emissions estimated with the three methods

344 OBB emissions estimated with the traditional bottom-up method for 2005-2012
345 were shown in Table [S8-S9](#) in the supplement. As emission factors were assumed
346 unchanged during the period, similar inter-annual trends were found for all species
347 and CO₂ was selected as a representative species for further discussion. As shown in
348 Figure 3, CO₂ emissions from traditional bottom-up method were estimated to
349 decrease from 23000 in 2005 to 19973 Gg in 2012, with a peak value of 27061 Gg in
350 2008. In contrast, the number of fire points in YRD farmland increased from 7158 in
351 2005 to 17074 in 2012. The fire counts detected from satellite thus did not support the
352 effectiveness of OBB restriction by government in YRD before 2013. Table [S9-S10](#) in
353 the supplement presents the annual OBB emissions derived from FRP-based method
354 for 2005-2015 in YRD region. Associated with fire counts, CO₂ emissions were
355 estimated to grow by 119.7% from 2005 to 2012, with the largest and the second
356 largest annual emissions calculated at 19977 and 12718 Gg for 2012 and 2010,
357 respectively (Figure 3). Similar temporal variability was found for fire counts, which
358 increased by 138.5% from 2005 to 2012, with the most and the second most counts
359 found at 17074 and 12322 for 2012 and 2010, respectively.

361 With the constraining method, as shown in Figure [S54](#) in the supplement, the
362 ratio of constrained mass of CRBF for 2012 to 2010 was 1.51, clearly lower than the
363 ratios of original FRE (1.75) but close to the ratio of modified FRE for 2012 to 2010
364 (1.57). The comparison suggested that modified FRE better reflect the OBB activity
365 in YRD than original FRE. In order to make the ratio of FRE for the two years be
366 closer to the ratio of constrained mass of CRBF, an improved method was developed
367 for calculating the FRE. Given the possible variation of FRP_{peak} hour between years,
368 we obtained the diurnal cycle of total FRP of YRD [for 2005-2015](#) based on Gaussian
369 fitting as shown in Figure [S65](#) in the supplement. The ratio of FRE for 2012 to 2010
370 was recalculated at 1.54, further closer to the ratio of constrained mass of CRBF.
371 Therefore the ratios of FRE for another given year to 2012 and 2010 were calculated
372 with this improved method, and were then applied to emission scaling for that year.
373 The constrained OBB emissions from 2005 to 2015 were summarized in Table 1. The
374 inter-annual trend in constrained emissions was similar with those in fire counts and

375 FRP-based emissions but different from that in emissions with traditional bottom-up
376 method, as shown in Figure 3. It is usually difficult to collect accurate percentages of
377 CRBF from bottom-up method, as it demands intensive investigation in the rural areas.
378 In addition, the percentages of CRBF were not updated for each year, and same
379 percentages were commonly applied for years without sufficient data support from
380 local surveys.

381 The constrained CO₂ emissions for Jiangsu, Anhui, Zhejiang and Shanghai were
382 calculated at 5790, 4699, 1104 and 419 Gg in 2005, accounting for 48.2%, 39.1%,
383 9.2% and 3.5% of total OBB emissions in YRD, respectively. The analogue numbers
384 for 2012 were 7345, 16159, 2574 and 394 Gg, and 27.7%, 61.0%, 9.7% and 1.5%,
385 respectively. Jiangsu and Anhui were found to contribute largest to OBB emissions in
386 YRD for 2005 and 2012, respectively. In the traditional bottom-up method, however,
387 Anhui was estimated to contribute largest for both years. City-level OBB emissions
388 | estimated with the three methods were summarized in Table [S10-S11-S12-S13](#) in the
389 supplement. With the constraining method, in particular, largest CO₂ emissions were
390 found in Suzhou (1708 Gg) of Anhui, Lianyungang (1578 Gg) and Xuzhou (1401 Gg)
391 of Jiangsu in 2005, accounting for 14.2%, 13.1% and 11.7% of the total emissions,
392 respectively. In 2012, Suzhou, Bozhou of Anhui, and Xuzhou of Jiangsu were
393 identified as the cities with the largest emissions, with the values estimated at 5007,
394 2433, and 2109 Gg, respectively. Depending on distribution of fire points, the shares
395 of OBB emissions by city were close between constraining and FRP-based method,
396 and large emissions concentrated in the north of YRD. Based on surveyed percentages
397 of CRBF and crop production, in contrast, the emission shares by city in traditional
398 bottom-up method were clearly different from the other two, and emissions
399 concentrated in Anhui cities with high crop production level.

400 The average annual emissions of CO₂ for 2005-2011 with traditional bottom-up
401 method were 87.0% larger than those in constraining method and the emissions for
402 2012 was 24.6% times smaller than those in constraining method. Given the same
403 sources of emission factors for all species except NMVOCs, the discrepancies of OBB
404 emissions for most species between constraining and traditional bottom-up methods
405 come from the activity levels (i.e., percentages of CRBF and crop production). The
406 average annual constrained emissions from 2005 to 2015 were larger than those
407 derived by FRP-based method for all species except EC, CH₄ and NH₃, since the

408 average annual mass of CRBF from constraining method were 36.9% larger than
409 those from FRP-based method for these years, as shown in Figure S76.

410 The percentage of CRBF is an important parameter to judge OBB activity and to
411 estimate emissions. Besides the investigated values applied in traditional bottom-up
412 approach, the percentages of CRBF were recalculated based on the constrained
413 emissions at provincial level and were shown in Figure S7-S8 in the supplement. The
414 largest and smallest percentages of CRBF in the whole YRD region were estimated at
415 18.3% in 2012 and 8.1% in 2006, respectively. The inter-annual trend in percentages
416 of CRBF for YRD was closest to that for Anhui province, as the province dominated
417 the crop burning in the region. The different inter-annual trends by province were
418 strongly influenced by agricultural practice and government management.
419 Agricultural practice could be associated with income level and mechanization level.
420 Increased income, would lead to more crop residues discarded and burned in the field,
421 while development of mechanization would lead to less. The constrained percentages
422 of CRBF for Shanghai increased from 2005 to 2007 and declined after 2007, while
423 those for Jiangsu decreased from 2005 to 2008 and increased after 2008. Increasing
424 trends were found for the percentages of CRBF for Anhui and Zhejiang from 2005 to
425 2012, and they might result largely from growth of farmers' income. Note that
426 percentages of CRBF for all provinces except Zhejiang decreased significantly in
427 2008, attributed largely to the measures of air quality improvement for Beijing
428 Olympic Games. Shanghai was the only one with its percentage of CRBF
429 significantly reduced in 2010, resulting mainly from the air pollution control for
430 Shanghai World Expo in that year. Compare to the percentages of CRBF used in
431 bottom-up method, the constrained ones of Anhui and Jiangsu for all the years except
432 2012 were smaller, leading to lower constrained OBB emissions than bottom-up ones
433 in those years.

434 The constrained percentages of CRBF and straw yields for 2012 were shown by
435 city in Figure S8-S9 in the supplement, and clear inconsistency in spatial distributions
436 can be found. The percentage of CRBF was not necessarily high for a city with large
437 straw production. For instance, straw production of Yancheng was higher than most
438 other cities, but its percentage of CRBF was 5.7% and lower than most other cities.
439 Through linear regression, correlation coefficient was calculated at only 0.06 between
440 constrained percentage of CRBF and straw yield at city level. The poor correlation
441 between them thus suggested that large uncertainty could be derived if uniform

442 percentage of CRBF was applied to calculate OBB emissions for cities within given
443 province, as what we did in the traditional bottom-up methodology.

444 **3.2 Evaluation of the three OBB inventories with CMAQ**

445 Figures 4 and 5 illustrate the observed 24-hour averaged and simulated hourly
446 PM₁₀ concentrations for selected YRD cities in June 17-25, 2010 and June 8-14, 2012,
447 respectively. Four emission cases, i.e., inventory without and with OBB emissions
448 estimated using the three methods, were included. The simulated PM₁₀ concentrations
449 without OBB emissions were significantly lower than observation for all cities,
450 implying that OBB was an important source of airborne particulates during the two
451 periods. Simulations with OBB emissions derived from the three methods performed
452 better than those without OBB emissions for most cities during June 17-25, 2010 and
453 all cities during June 8-14, 2012. The best performance was found for simulations
454 with constrained OBB emissions in most cities during the two periods, and the high
455 PM₁₀ concentrations were generally caught by CTM for the concerned OBB events. In
456 2010, the observed high concentrations were simulated with constrained emissions in
457 Lianyungang during June 21-23, and Fuyang and Huainan during June 19-21. In 2012,
458 the observed high concentrations were caught with constrained emissions in Xuzhou
459 during June 12-14, Lianyungang during June 13-14, Fuyang during June 11-12,
460 Bozhou during June 10 and Chuzhou during June 11-12. The results thus indicated
461 that fire points could principally capture the temporal and spatial distribution of OBB
462 emissions. Overestimation still existed with constrained OBB emissions for the cities
463 with intensive fire points (e.g., Xuzhou, Bozhou and Fuyang in 2012 and Bengbu in
464 2010), while underestimation commonly existed for cities with fewer fire points (e.g.,
465 Hefei, Chuzhou and Huainan in 2010 and 2012). Due to limitation of MODIS
466 observation, fires at moderate to small scales could not be fully detected (Giglio et al.,
467 2003; Schroeder et al., 2008), thus the spatial allocation of OBB emissions based on
468 FRP could possibly result in more emissions than actual in areas with intensive fire
469 points. In order to further evaluate the OBB emissions, Moreover, we used both
470 PM_{2.5} and PM₁₀ concentrations (which were available since 2013) to evaluate the
471 model performances when the constrained, FRP-based or no OBB emissions based
472 on constraining and FRP-based methods and without OBB emissions were applied in
473 CTM for during OBB event of during June 7-13, 2014. Figures S10 and S11 in the
474 supplement illustrate the observed and simulated hourly concentrations for PM_{2.5} and

475 PM₁₀ concentrations for in selected YRD cities on June 7-13, 2014, respectively. The
476 best performance was found for simulations with the constrained OBB emissions in
477 most cities during the periods, and the high PM_{2.5} and PM₁ peak particle₀
478 concentrations were generally caught by CTM for the concerned OBB events. The
479 observed high concentrations were simulated with the constrained emissions in
480 Lianyungang and Suqian during on June 12 and Huaian and Yancheng during on June
481 13.

482 The NMB and NME between observed and simulated PM_{2.5} and PM₁₀
483 concentrations are shown in Table 2. ~~Among all~~In most the cases, the NMB and NME
484 with constrained OBB emissions were smaller than ~~most of~~ those with other OBB
485 emissions, implying the best guess of OBB emissions obtained through the
486 constraining method combining CTM and ground observation. The simulated PM_{2.5}
487 and PM₁₀ concentrations using FRP-based OBB emissions were smaller than
488 observation for the ~~threetwo~~ periods, due mainly to the mass of CRBF were
489 underestimated. The results thus indicated that OBB emissions might be
490 underestimated in FRP-based method in 2010, 2012 and 20142, since many small
491 fires in YRD were undetected in MODIS active fire detection products. The
492 probability of MODIS detection was strongly dependent upon the temperature and
493 area of the fire being observed. The average probability of detection for tropical
494 savanna was 33.6% when the temperature of fire was between 600 and 800 °C and the
495 area of fire was between 100 and 1000 m² (Giglio et al., 2003). In YRD region, on
496 one hand, the fire temperature of crop residue burned in fields was relatively low. On
497 the other hand, nearly 100 farmers were possibly located in a single 1 × 1 km MODIS
498 pixel (Liu et al., 2015), and a famer commonly owned croplands of several hundred
499 square meters. Therefore many fire pixels in YRD might not be detected, leading to
500 underestimation in the total FRE. The simulated PM₁₀ concentrations using traditional
501 bottom-up OBB emissions were higher than observation in 2010 but lower in 2012.
502 The results thus implied the growth in OBB emissions from 2010 to 2012 could not
503 be captured by traditional bottom-up method, attributed partly to application of
504 unreliable percentage of CRBF. We further selected the performance of CMAQ
505 modeling in US (Zhang et al., 2006) as the benchmark for PM_{2.5} and PM₁₀ simulation.
506 As can be seen in Table 2, the NMBs and NMEs for most case with the constrained
507 OBB emissions were close to those by Zhang et al. (2006). The NMEs for hourly

带格式的：字体：Times New Roman

带格式的：字体：Times New Roman

带格式的：字体：Times New Roman

508 PM_{2.5} and PM₁₀ were slightly larger. Given the larger uncertainty in emission
509 inventory of anthropogenic sources for China and the uncertainty in spatial and
510 temporal distribution of OBB emissions due to satellite detection limit, we believe the
511 model performance with the constrained OBB emissions was improved and
512 acceptable.

513 The NMB of hourly PM_{2.5} and PM₁₀ during OBB event of June 2014 with
514 constrained OBB emissions were smaller than those of Zhang (2006), and the NME of
515 hourly PM_{2.5} and PM₁₀ with constrained OBB emissions were larger than those of
516 Zhang (2006). Considering that the accuracy of emissions of other sources for US
517 might be higher than that used in this study and there were uncertainties in the
518 temporal and spatial distribution of OBB emissions derived from satellite due to
519 insufficient satellite detection capability, the model performance with constrained
520 OBB emissions was acceptable. However, the NMB and NME of hourly PM_{2.5} and
521 PM₁₀ without OBB emissions and with FRP-based emissions were higher than those
522 of Zhang (2006).

523

524 **3.3 Comparisons of different methods and studies**

525 We selected CO to compare emissions in this work and other inventories for
526 YRD, given the similar emission factors of CO applied in different studies. CO
527 emissions from the three methods in this study were compared with GFASv1.0
528 (Kaiser et al., 2012), GFEDv3.0 (van der Werf et al., 2010), GFEDv4.1 (Randerson et
529 al. [20152018](#)), Wang and Zhang (2008), Huang et al. (2012), Xia et al. (2016) and
530 Zhou et al. (2017a), as shown in Figure 6. The emissions from Wang and Zhang
531 (2008), Huang et al. (2012), Xia et al. (2016) and Zhou et al. (2017a) were derived by
532 traditional bottom-up method, while GFASv1.0, GFEDv3.0 and GFEDv4.1 were
533 based on FRP and BA methods. In particular, emissions from small fires were
534 included in GFEDv4.1. Similar inter-annual variations were found for emissions
535 derived from FRP measurement including the constrained and FRP-based emissions
536 in this work, GFAS v1.0, and GFED v4.1, while those of GFEDv3.0 and Xia et al.
537 (2016) were different. The percentages of CRBF were assumed unchanged during the
538 studying period in Xia et al. (2016), thus the temporal variation of OBB emissions
539 were associated with the change in annual straw production.

540 The constrained CO emissions in this work were lower than other studies using
541 traditional bottom-up method (Wang and Zhang, 2008; Huang et al., 2012; Xia et al.,
542 2016) and higher than those based on burned area and FRP derived from satellite
543 (GFEDv3.0; GFASv1.0; GFEDv4.1). In particular, the average annual constrained
544 emissions from 2005 to 2012 were 3.9, 0.5 and 15.0 times larger than those in
545 GFASv1.0, GFEDv4.1s and GFEDv3.0, respectively. The constrained emissions were
546 closest to GFED v4.1s that included small fires. Since the area of farmland belonging
547 to individual farmers was usually small, small fires were expected to be important
548 sources of OBB emissions in YRD. GFEDv4.1s might still underestimate OBB
549 emissions due to the omission errors for the small fires in MODIS active fire detection
550 products (Schroeder et al., 2008). In addition, the constrained CO emission for 2013
551 was 31.5% larger than those by Qiu et al. (2016) calculated based on burned area from
552 satellite observations. The average annual CO emissions from 2005 to 2012 by the
553 constraining method were 57.2% smaller than Xia et al. (2016), and the constrained
554 emissions for 2006 were respectively 27.6% and 56.9% lower than those by Huang et
555 al. (2012) and Wang and Zhang (2008). It implied again that the emissions derived
556 from traditional bottom-up method might be overestimated. Moreover, discrepancy in
557 estimations for the same year between Huang et al. (2012) and Wang and Zhang
558 (2008) with traditional bottom-up resulted mainly from application of different
559 percentages of CRBF, implying that calculation of OBB emissions was sensitive to
560 the parameter with the bottom-up approach.

561 The spatial distribution of constrained emissions in this work and those in
562 GFASv1.0, GFEDv3.0 and GFEDv4.1s were illustrated in Figure 7. Intensive OBB
563 emissions in GFEDv3.0 were mainly found in parts of Anhui, Jiangsu and Shanghai,
564 while the constrained emissions, GFEDv4.1s and GFASv1.0 emissions occurred in
565 most YRD regions in accordance with the distribution of fire points. Therefore,
566 GFEDv3.0 might miss a large number of burned areas, leading to underestimation in
567 emissions and bias in spatial distribution.

568 In order to understand the discrepancies of emissions for different species in this
569 work and other inventories, the emissions of 2010 derived from the three methods in
570 this study, GFASv1.0, GFEDv3.0, GFEDv4.1s and Xia et al. (2016) were summarized
571 in Table 3. Similar to CO, the constrained emissions for all species in this work were
572 lower than Xia et al. (2016) and OBB emissions of this study based on traditional
573 bottom-up method. The constrained emissions for all species in this work were larger

574 than GFASv1.0 and those for all species except NH₃ were larger than GFEDv3.0 and
575 GFEDv4.1s. In addition, the constrained emissions for most species were lower than
576 the emissions from Huang et al. (2012), Wang and Zhang (2008) and Xia et al. (2016)
577 using traditional bottom-up method in 2006. In most cases, the discrepancy in activity
578 levels between studies was larger than that in emission factors. Specifically, the OBB
579 emissions for all species— in FRP-based (WSE) with same emission factors as
580 bottom-up method based on FRP based method were lower smaller than those derived
581 by bottom-up method. The differences in OBB emissions between bottom-up and
582 FRP-based (WSE) method were larger than 50% of those between the bottom-up and
583 the original FRP-based method with different emission factors for most species. The
584 differences of in OBB emissions for most species between bottom up and FRP based
585 method with same emission factors (WSE) were larger than or half more than those
586 between bottom up and FRP based method with different emission factors. It
587 indicated that the discrepancy in activity levels contributed the most of to the
588 difference of in OBB emissions between bottom-up and FRP-based the two methods.

589 Resulting from the different sources of emission factors, the discrepancies
590 between studies or methods varied greatly by species. For PM₁₀ and PM_{2.5}, as an
591 example, the emissions by Xia et al. (2016) were respectively 35.8% and 50.3%
592 higher than constrained emissions in 2010. The discrepancies for SO₂ and NO_x were
593 larger: the emissions by Xia et al. (2016) were 4.7 and 3.1 times larger than our
594 constrained emissions, respectively. Moreover, the constrained NMVOCs emission
595 was 152.5 and 10.7 times larger than that of GFEDv3.0 and GFEDv4.1s in 2010, as
596 the emission factors of GFEDv3.0 and GFEDv4.1s did not contain oxygenated VOCs.
597 In contrast, the constrained NH₃ emission was 4.7% and 47.9% smaller than that of
598 GFEDv3.0 and GFEDv4.1s. The comparisons indicated that emission factors were
599 important sources of uncertainties in estimation of OBB emissions with different
600 methods.

601 **3.4 Contribution of OBB to particulate pollution and its influencing factors**

602 The brute-force method (BFM, Dunker et al., 1996) was used to analyze the
603 contributions of OBB to ~~particulate-PM₁₀~~ pollution for the two OBB events, June
604 17-24, 2010 and June 8-14, 2012. Simulated PM₁₀ concentrations with and without
605 constrained OBB emissions were compared, and the difference indicated the
606 contribution from OBB as shown by city in Figure 8. The average contribution in June

带格式的：下标

607 8-14, 2012 was estimated at 37.6% ($56.7 \mu\text{g}/\text{m}^3$) for 22 cities in YRD, and the
608 contribution for June 17-24, 2010 was smaller at 21.8 % ($24.0 \mu\text{g}/\text{m}^3$) for 17 cities.
609 Our result for 2012 was nearly the same as that for 5 YRD cities in 2011 (37.0%) by
610 Cheng et al. (2014). Using the BFM method, the contribution of OBB emissions to
611 PM_{10} concentrations were estimated to increase by 136.3% from 2010 to 2012 in this
612 work, and the growth rate was larger than that of OBB emissions (50.8%). Therefore,
613 factors other than emissions (e.g., meteorology) could also play an important role in
614 elevating the contribution of OBB to ambient particle pollution. For example, the
615 average precipitation in June 8-14, 2012 was 36% lower than that in June 17-24, 2010,
616 exaggerating the particle pollution during OBB event. For the OBB event during June
617 7-13, 2014, in order to know the contributions of OBB to both $\text{PM}_{2.5}$ and PM_{10}
618 pollution during OBB event, the brute force method was used to analyze the
619 contributions of OBB to $\text{PM}_{2.5}$ and PM_{10} in June 7-13, 2014, and the contributions
620 from OBB to both $\text{PM}_{2.5}$ and PM_{10} concentrations were shown by city in Figure 9.
621 The average contributions of $\text{PM}_{2.5}$ and PM_{10} in June 7-13, 2014 were estimated at
622 29.3% ($20.0 \mu\text{g}/\text{m}^3$) and 23.1% ($17.3 \mu\text{g}/\text{m}^3$) for 22 cities in YRD, indicating again-
623 Therefore, the contribution of OBB to PM_{10} was up to 78.8% of the contribution of
624 OBB to $\text{PM}_{2.5}$. It suggested that the OBB was an important source of $\text{PM}_{2.5}$ and
625 PM_{10} ambient particles simultaneously. The O-BB contributions of to PM_{10} for 2014
626 was obviously smaller than that of for 2012 and close to that of 2010, attributed mainly
627 due mainly to the reduced straw burning in crop land. difference of OBB emissions.

628 The average contributions of OBB for 2012 were estimated at 55.0% (98.4
629 $\mu\text{g}/\text{m}^3$), 36.4% ($58.0 \mu\text{g}/\text{m}^3$), 23.6% ($12.9 \mu\text{g}/\text{m}^3$), and 14.4% ($11.2 \mu\text{g}/\text{m}^3$) for 6
630 cities of Anhui, 10 cities of Jiangsu, 5 cities of Zhejiang and Shanghai, respectively.
631 For individual cities, large contributions of OBB for 2012 were found in Xuzhou,
632 Bozhou, Fuyang, and Lianyungang located in the north YRD, reaching 82.3% (284.3
633 $\mu\text{g}/\text{m}^3$), 75.2% ($207.5 \mu\text{g}/\text{m}^3$), 71.9% ($134.7 \mu\text{g}/\text{m}^3$) and 63.5% ($96.2 \mu\text{g}/\text{m}^3$),
634 respectively. Similarly, large contributions for 2010 were found in Lianyungang,
635 Fuyang and Bozhou reaching 63.3% ($69.8 \mu\text{g}/\text{m}^3$), 58.2% ($71.9 \mu\text{g}/\text{m}^3$) and 78.8%
636 ($53.6 \mu\text{g}/\text{m}^3$), respectively. In general the spatial distribution of contributions to PM_{10}
637 mass concentrations was similar with that of fire points, confirming the rationality of
638 constraining OBB emissions with observed PM_{10} concentration in cities in north
639 Anhui and Jiangsu. The similar result was found in For contributions of OBB to
640 $\text{PM}_{2.5}$ during the OBB event in 2014, the large contributions of OBB were found in

带格式的：下标

带格式的：下标

641 [Xuzhou, Huaian and Suqian located in the in the north YRD during the event in 2014,](#)
642 [reaching 67.5% \(111.7 \$\mu\text{g}/\text{m}^3\$ \), 60.7% \(50.6 \$\mu\text{g}/\text{m}^3\$ \) and 53.2% \(49.6 \$\mu\text{g}/\text{m}^3\$ \),](#)
643 [respectively.](#)

644 To explore the influence of meteorology on air pollution caused by OBB, we
645 simulated PM_{10} concentrations for June 8-14 (PE1) and June 22-28 2012 (PE2) with
646 varied meteorology conditions but fixed OBB emissions (i.e., constrained emissions
647 for June 8-14, 2012). Poorer meteorology conditions during PE1 were found than PE2.
648 The average wind speed in PE1 was 2.4 m/s, 17% lower than that in PE2. The average
649 wind direction in PE1 was 168.3° , close to south with polluted air in land. In contrast,
650 the average wind direction in PE2 was 118.3° , close to east with clean air from the
651 ocean. The average precipitation in PE2 was 6.8mm, 28% higher than that in PE1. As
652 shown in Figure 910, the average contribution of OBB to PM_{10} concentrations for 22
653 cities in YRD region was estimated at $56.7 \mu\text{g}/\text{m}^3$ for PE1, 23% larger than that for
654 PE2, and the contributions in most cities were much larger for PE1 than those for PE2,
655 except for Bozhou and Fuyang. The comparisons thus suggest that air pollution
656 caused by OBB would exaggerate under poorer meteorology conditions. To reduce air
657 pollution caused by OBB in harvest season in YRD, therefore, more attention should
658 be paid to the OBB restriction on those days with unfavorable meteorology conditions
659 such as calm wind and rainless period.

660 To further analyze the influence of diurnal variation of emissions on air pollution
661 caused by OBB, we simulated PM_{10} concentrations of June 17-24 2010 with various
662 diurnal curves of OBB emissions (i.e., those for 2010 and 2012). Constrained
663 emissions were applied in the simulation. As shown in Figure 4011, the contributions
664 of OBB to PM_{10} concentrations based on diurnal curve of 2012 were larger than those
665 based on 2010 for almost all YRD cities, and the average contribution for the 17 cities
666 was calculated at $28.6 \mu\text{g}/\text{m}^3$ based on diurnal curve of 2012, 10% larger than that
667 based on 2010. The contribution in Bozhou changed most (1.37 times larger with
668 2012 curve), while those in Shanghai, Huzhou and Shaoxing changed least. The time
669 of peak value for OBB emissions in 2012 was 2.5 hours later than 2010, indicating
670 that the fraction of OBB emissions at night for 2012 would be larger than that for
671 2010. As the diffusion condition for air pollutants at night was usually worse than that
672 during daytime, more OBB emissions at night would elevate its contribution to
673 particle pollution. In the actual fact, the supervision of OBB prohibition was usually
674 conducted by government during daytime, thus some farmers burned more crop

675 residues at night to avoid the punishment. To improve the air quality in harvest season
676 in YRD, more attention should be paid to the OBB restriction at night.

677 **3.5 Uncertainty analysis**

678 The uncertainties of OBB emissions estimated with bottom-up and FRP-based
679 methods were quantified by species using a Monte-Carlo simulation for 2012. A total
680 of 20,000 simulations were performed and the uncertainties were expressed as 95%
681 confidence intervals (CIs) around the central estimates. The parameters contributing
682 most to OBB emission uncertainty were also identified according to their contribution
683 to the variance in Monte-Carlo simulation.

684 For traditional bottom-up method, parameters included crop productions,
685 percentages of CRBF, straw to grain ratios, combustion efficiencies, and emission
686 factors. Crop production was directly taken from official statistical yearbooks (NBS,
687 2013) and its uncertainty was expected to be limited and not included in the analysis.
688 As the percentage of CRBF was determined at half of the percentage of unused crop
689 residues, its uncertainty was set at -100% to +100%. The combustion efficiencies
690 were assumed within an uncertainty range of 10% around the mean value according to
691 de Zarate (2005) and Zhang et al. (2008). Uncertainties of emission factors were
692 obtained from original literatures where they were derived. If emission factor was
693 derived from a single measurement, normal distribution was applied with standard
694 deviation directly taken from that work. If emission factor was derived from multiple
695 measurements and the samples were insufficient for data fitting, uniform distribution
696 was tentatively applied with a conservative strategy to avoid possible underestimation
697 of uncertainty: The uncertain range of given emission factor would be expanded
698 according to Li et al. (2007) if the range originally from multiple studies was smaller
699 than that in Li et al. (2007). Summarized in Table [S13-S14](#) in the supplement was a
700 database for emission factors and percentages of CRBF, with their uncertainties
701 indicated by probability distribution function (PDF). As shown in Table 4, the
702 uncertainties of OBB emissions with traditional bottom-up method for PM₁₀, PM_{2.5},
703 EC, OC, CH₄, NMVOCs, CO, CO₂, NO_x, SO₂ and NH₃ in 2012 were estimated at
704 -56% to +70%, -56% to +70%, -50% to +54%, -54% to +73%, -49% to +58%, -48%
705 to +59%, -46% to +73%, -48% to +60%, -47% to +87%, -59% to +138% and -51% to
706 +67%, respectively. For most species, the percentages of CRBF contributed largest to

707 the uncertainties of OBB emissions, while emission factors were more significant to
708 SO₂ uncertainty.

709 For FRP-based method, parameters included total FRE, combustion conversion
710 ratio and emission factors. Uncertainty of total FRE was associated with FRP value,
711 MODIS detection resolution, and the methodology used to calculate FRE per fire
712 pixel. Indicated by Freeborn et al. (2014), the coefficient of variation of MODIS FRP
713 for a fire pixel was 50%, but it declined to smaller than 5% for the aggregation of over
714 50 MODIS active fire pixels. Give the large number of fire pixels for in YRD (more
715 than 17000 in 2012), FRP was expected to contribute little to uncertainty of total FRE
716 and could thus be ignored. Due to limitation of MODIS resolution, small fires could
717 not be fully detected and the number of fire pixel could be underestimated by 300%
718 on crop-dominant areas (Schroeder et al., 2008), therefore the uncertainty of number
719 of fire pixel was assumed to be 0 to +300%. The method used to calculate FRE based
720 on single fire pixel assumed that fire lasted one day. Given the small cropland owned
721 by one farmer in YRD, individual fire normally lasted several hours, and FRE could
722 be overestimated. As the total FRE in FRP-based method was estimated 2.6 times
723 larger than that from constraining method based on the same number of the fire pixel,
724 we tentatively assumed the uncertainty range of FRE for one fire pixel at 0% to -72%.
725 The uncertainty of total FRE was then estimated at -17% to +154% (95% CIs) based
726 on the principle that total FRE was calculated as the number of fire pixel multiplied
727 by average FRE. The uncertainty of combustion conversion ratio was derived from
728 Wooster et al. (2005) and Freeborn et al. (2008), while those of emission factors taken
729 from Akagi et al. (2011). As a result, uncertainties of FRP-based inventory were
730 estimated at -77% to +274%, -63% to +244%, -78% to +281%, -78% to 276%, -83%
731 to +315%, -63% to +243%, -52% to +223%, -21% to +164%, -82% to +303%, -78%
732 to +279%, and -82% to +302% for PM₁₀, PM_{2.5}, EC, OC, CH₄, NMVOCs, CO, CO₂,
733 NO_x, SO₂ and NH₃ in 2012, respectively. Emission factors contributed most to the
734 uncertainties of emissions for all species except CO₂.

735 The uncertainty of constrained emissions could hardly be provided by
736 Monte-Carlo simulation, as the results were associated with CTM performance. In
737 general, CTM performance could be influenced by emission estimates for sources
738 other than OBB, chemistry mechanism of CTM and temporal and spatial distribution
739 of OBB emissions. Emission inventory of anthropogenic sources that incorporates the
740 best available information of individual plants was expected to improve the CTM

741 performance at the regional or local scale (Zhou et al., 2017b). The influence of
742 chemistry mechanism came mainly from secondary organic carbon (SOC) modeling.
743 According to the Cheng et al. (2014) and Chen et al. (2017), the mass fraction of SOC
744 to PM₁₀ could reach 10% during the OBB event in YRD, and that part might not be
745 well constrained with the approach we applied in this work. Similar to FRP-based
746 method, moreover, temporal and spatial distribution of OBB emissions based on FRP
747 might not be entirely consistent with the reality, due to omission errors in the MODIS
748 active fire detection products and limited times of satellite overpass as discussed
749 earlier. Due to data limitation, finally, we relied on available PM₁₀ concentrations in
750 current method. More data of multi pollutant concentrations (e.g., PM_{2.5}, OC and EC)
751 with sufficient temporal and spatial resolution are in great need to better constrain the
752 OBB emissions.

带格式的: 下标

带格式的: 下标

753 In general, uncertainties of OBB emissions with traditional bottom-up method
754 were estimated smaller than those with FRP-based method, and uncertainties for CO₂
755 and CO were usually smaller than other species in both methods attributed mainly to
756 fewer variations in their emission factors. OBB emission estimation with traditional
757 bottom-up method could be improved if more accurate percentages of CRBF are
758 obtained, and that with FRP-based method could be improved when the omission
759 error of satellite and the uncertainties of emission factors are reduced. Efforts should
760 also be recommended on improvement of CTM for better constraining the OBB
761 emissions.

762

763 4. Conclusions

764 Taking YRD in China as an example, we have thoroughly analyzed the
765 discrepancies and their sources of OBB emissions estimated with traditional
766 bottom-up, FRP-based and constraining methods. The simulated PM₁₀ concentrations
767 through CMAQ with constrained emissions were closest to available observation,
768 implying the improvement of emission estimation with this method. The inter-annual
769 variations in emissions with FRP-based and constraining methods were similar with
770 the fire counts, while that with traditional bottom-up method was not. It indicated that
771 emissions with traditional bottom-up method could not capture the real inter-annual
772 trend of OBB emissions. The emissions of all species except NMVOCs based on
773 traditional bottom-up method might be overestimated in most years, attributed mainly

774 to the elevated percentages of CRBF used in the method. The emissions with
775 FRP-based method might be underestimated in 2005-2015, attributed to the omission
776 errors in the MODIS active fire detection products and thereby to the underestimation
777 in mass of CRBF. The CO emissions with traditional bottom-up, FRP-based and
778 constraining methods were compared with other studies. Similar temporal variations
779 were found for the constrained emissions, emissions based on FRP-based, and
780 emissions in GFASv1.0 and GFEDv4.1s. CO emissions based on traditional
781 bottom-up method both in this work and other studies were usually higher than those
782 derived by constraining method, and the CO emissions based on FRP-based method
783 both in this work and other studies usually were lower than those derived by
784 constraining method. It again demonstrated that traditional bottom-up method might
785 overestimate OBB emissions in YRD and FRP-based method might underestimate
786 them. The contributions of OBB to particulate pollution in typical episodes were
787 analyzed using the Brute-force method in CMAQ modeling. The OBB emissions in
788 2012 were 51% larger than those in 2010, while its contribution to average PM₁₀ mass
789 concentrations was estimated to increase by 136% from 2010 to 2012. It indicated that
790 the elevated contribution of OBB was not attributed only to growth in OBB emissions
791 but was also influenced by the meteorology. Quantified with a Monte-Carlo
792 framework, the uncertainties of OBB emissions with traditional bottom-up method
793 were smaller than those with FRP-based method. The uncertainties of emissions based
794 on traditional bottom-up and FRP-based were mainly from the percentages of CRBF
795 and emission factors, respectively. Further improvement on CTM for OBB events
796 would help better constraining OBB emissions.

797 Limitations remained in this study. Given the difficulty in field investigation,
798 annual CRBF used in traditional bottom-up method was obtained from limited studies
799 and it could not correctly reflect the real OBB activity. The reliability of OBB
800 emissions with FRP-based method depended largely on the detection resolution of the
801 satellite. In YRD where the burned areas of individual fires were small, many fires
802 could not be detected by MODIS. The accuracy of constrained emissions depended
803 largely on model performance and spatial and temporal distributions of OBB
804 emissions derived from satellite-observed FRP. Therefore FRP-based and constraining
805 method may be improved if more reliable fire information is obtained. In addition,
806 more measurements on local emission factors for OBB are suggested in the future to
807 reduce the uncertainty of emissions.

808

809

Acknowledgements

810 This work was sponsored the National Key Research and Development Program
811 of China (2016YFC0201507 and 2017YFC0210106), Natural Science Foundation of
812 China (91644220 and 41575142), Natural Science Foundation of Jiangsu
813 (BK20140020), and Special Research Program of Environmental Protection for
814 Common wealth (201509004). The MCD14ML data were provided by LANCE
815 FIRMS operated by the NASA/GSFC/Earth Science Data and Information System
816 (ESDIS) with funding provided by NASA/HQ.

817

818

References

- 819 Akagi, S., Yokelson, R. J., Wiedinmyer, C., Alvarado, M., Reid, J., Karl, T., Crounse,
820 J., and Wennberg, P.: Emission factors for open and domestic biomass burning for use
821 in atmospheric models, *Atmos. Chem. Phys.* 11 (9), 4039-4072, 2011.
- 822 Andreae, M. O., and Merlet, P.: Emission of trace gases and aerosols from bio
823 mass burning, *Glob. Biogeochem. Cy.* 15(4), 955-966. <http://dx.doi.org/10.1029/2000gb001382>, 2001.
- 825 Bi, Y. Y.: Study on straw resources evaluation and utilization, Chinese Academy
826 Agriculture Sciences, Beijing, China, 2010 (in Chinese).
- 827 Cao, G. L., Zhang, X. Y., Wang, D., and Zheng, F. C.: Inventory of atmospheric
828 pollutants discharged from open biomass burning in China continent, *Chinese Science*
829 *Bulletin*, 52(15):1826-1831, 2007 (in Chinese).
- 830 Chen, D., Cui H. F., Zhao Y., Yin L., Lu, Y., Wang, Q. G.: A two-year study of
831 carbonaceous aerosols in ambient PM 2.5 at a regional background site for western
832 Yangtze River Delta, China, *Atmos. Res.*, 183, 351-361, 2017.
- 833 Cheng, Z., Wang, S.X., Fu, X., Watson, J.G., Jiang, J., Fu, Q., Chen, C., Xu, B., Yu, J.,
834 Chow, J.C., and Hao, J.: Impact of biomass burning on haze pollution in the Yangtze
835 River delta, China: a case study in summer 2011, *Atmos. Chem. Phys.*, 14, 4573-4585,
836 2014.
- 837 Cheng, Z., Wang, S.X., Jiang, J. K., Fu, Q.Y., Chen, C.H., Xu, B.Y., Yu J.Q., Fu, X.,
838 and Hao J.M.: Long-term trend of haze pollution and impact of particulate matter in
839 the Yangtze River Delta, China, *Environ. Pollut.*, 182, 101-110, 2013.
- 840 Crutzen, P. J., and Andreae, M. O.: Biomass burning in the tropics: Impact on
841 atmospheric chemistry and biogeochemical cycles, *Science*, 250 (4988), 1669-1678,
842 1990.
- 843 Davies, D. K., Ilavajhala, S., Wong, M. M., and Justice, C. O.: Fire Information for
844 Resource Management System: Archiving and Distributing MODIS Active Fire Data,
845 *IEEE Geosci. Remote Sens.*, 47, 72-79, 2009.
- 846 de Zarate, I. O., Ezcurra, A., Lacaux, J. P., Van Dinh, P., de Argandona, J. D.:

847 Pollution by cereal waste burning in Spain, *Atmos. Environ.*, 73, 161~170, 2005.

848 Dunker, A. M., Morris, R. E., Pollack, A. K., Schleyer, C. H., and Yarwood, G.:
849 Photochemical modeling of the impact of fuels and vehicles on urban ozone using
850 auto oil program data, *Environ. Sci. & Technol.*, 30, 787–801, 1996.

851 [Emery, C., Tai, E., and Yarwood, G.: Enhanced meteorological modeling and
852 performance evaluation for two Texas episodes, Report to the Texas Natural
853 Resources Conservation Commission, prepared by ENVIRON, International Corp,
854 Novato, CA, 2001.](#)

855 European Space Agency and Université Catholique de Louvain, GLOBCOVER
856 2009 Products Description and Validation Report, 2011, Available online: [http://
857 due.esrin.esa.int/files/GLOBCOVER2009_Validation_Report_2.2.pdf](http://due.esrin.esa.int/files/GLOBCOVER2009_Validation_Report_2.2.pdf).

858 Fu, X., Wang, S.X., Zhao, B., Xing, J., Cheng, Z., Liu, H., and Hao, J. M.: Emission
859 inventory of primary pollutants and chemical speciation in 2010 for the Yangtze River
860 Delta region, China, *Atmos. Environ.*, 70, 39-50, 2013.

861 Freeborn, P. H., Wooster, M. J., Roy, D. P., Cochrane, M. A.: Quantification of
862 MODIS fire radiative power (FRP) measurement uncertainty for use in satellite based
863 active fire characterization and biomass burning estimation, *Geophys. Res. Lett.*,
864 41(6), 1988-1994, 2014.

865 Freeborn, P. H., Wooster, M. J., Hao, W. M., Ryan, C. A., Nordgren, B. L., Baker, S. P.,
866 and Ichoku, C.: Relationships between energy release, fuel mass loss, and trace gas
867 and aerosol emissions during laboratory biomass fires, *J. Geophys. Res.*, 113, D01301.
868 <http://dx.doi.org/10.1029/2007jd008679>, 2008.

869 Giglio, L., Randerson, J. T., and van der Werf, G. R.: Analysis of daily, monthly, and
870 annual burned area using the fourth generation global fire emissions database
871 (GFED4), *J. Geophys. Res.: Biogeo.*, 118, 317–328, doi:10.1002/jgrg.20042, 2013.

872 Giglio, L., Descloitres, J., Justice, C. O., Kaufman Y. J.: An enhanced contextual fire
873 detection algorithm for MODIS, *Remote Sens. Environ.*, 87(2-3): 273-282, 2003.

874 Guo, H., Cheng, T., Gu, X., Wang, Y., Chen, H., Bao, F., Shi, S. Y., Xu, B. R., Wang,
875 W. N., Zuo, X., Zhang, X. C., Meng, C.: Assessment of pm_{2.5} concentrations and
876 exposure throughout china using ground observations, *Sci. Total Environ.*, 1024,
877 601-602, 2017.

878 Hodzic A., Duvel J. P.: Impact of biomass burning aerosols on the diurnal cycle of
879 convective clouds and precipitation over a tropical island, *J. Geophys. Res.*, 123,
880 1017–1036. <https://doi.org/10.1002/2017JD027521>, 2018.

881 Hooghiemstra, P. B., Krol, M. C., vanLeeuwen, T. T., van der Werf, G. R., Novelli, P.
882 C., Deeter, M. N., Aben, I., and Röckmann, T.: Interannual variability of carbon
883 monoxide emission estimates over South America from 2006 to 2010, *J. Geophys.*
884 *Res.*, 117, D15308, doi:10.1029/2012JD017758, 2012.

885 Huang, X., Ding, A. J., Liu, L. X., Liu, Q., Ding, K., Nie, W., Xu, Z., Chi, X. G.,
886 Wang, M. H., Sun, J. N., Guo, W. D., and Fu, C. B.: Effects of aerosol-radiation
887 interaction on precipitation during biomass-burning season in East China, *Atmos.*
888 *Chem. Phys. Discuss.*, doi: 10.5194/acp-2016-272, 2016.

889 Huang, X., Li M., Li, J., Song, Y.: A high-resolution emission inventory of crop
890 burning in fields in China based on MODIS Thermal Anomalies/Fire products, *Atmos.*

- 带格式的: 字体: Times New Roman
- 带格式的: 字体: Times New Roman
- 带格式的: 字体: Times New Roman
- 带格式的: 定义网格后不调整右缩进, 无孤行控制
- 带格式的: 字体: Times New Roman
- 带格式的

936 Ran, L., Zhao, C., Geng, F., Tie, X., Peng, L., Zhou, G., Yu, Q., Xu, J., and
937 Guenther, A.: Ozone photochemical production in urban Shanghai, China: Anal
938 ysis based on ground level observations, *J. Geophys. Res.*, 114, D15301, doi: 10.
939 1029/2008JD010752, 2009.

940 Randerson, J. T., van der Werf, G. R., Giglio, L., Collatz, G. J., and Kasibhatla, P. S.:
941 Global Fire Emissions Database, Version 4.1, (GFEDv4), ORNL DAAC, Oak Ridge,
942 Tennessee, USA. <http://dx.doi.org/10.3334/ORNLDAAAC/1293>, 2015-2018.

943 Richter, A., Burrows, J. P., Nuss, H., Granier, C., and Niemeier, U.: Increase in
944 tropospheric nitrogen dioxide over China observed from space, *Nature*, 437, 129-132,
945 2005.

946 Schroeder, W., Prins, E., Giglio, L., Csiszar, I., Schmidt, C., Morisette, J., and
947 Morton, D.: Validation of GOES and MODIS active fire detection products usi
948 ng ASTER and ETM+ data, *Remote Sens. Environ.*, 112 (5), 2711-2726, [http://](http://dx.doi.org/10.1016/j.rse.2008.01.005)
949 dx.doi.org/10.1016/j.rse.2008.01.005, 2008.

950 Shi, Y. S., and Yamaguchi, Y.: A high-resolution and multi-year emissions inventory
951 for biomass burning in Southeast Asia during 2001-2010, *Atmos. Environ.*, 98 (98):
952 8-16, 2014.

953 Sindelarova, K., Granier, C., Bouarar, I., Guenther, A., Tilmes, S., Stavrakou, T.,
954 Müller, J.-F., Kuhn, U., Stefani, P., and Knorr, W.: Global data set of biogenic VOC
955 emissions calculated by the MEGAN model over the last 30 years, *Atmos. Chem.*
956 *Phys.*, 14, 9317-9341, doi: 10.5194/acp-14-9317-2014, 2014.

957 Streets, D. G., and Yarber, K. F.: Biomass burning in Asia: Annual and seasonal
958 estimates and atmospheric emissions, *Global Biogeochemical Cycles*, 17, 4, 1099, doi:
959 10.1029/2003GB002040, 2003.

960 Su, J. F., Zhu B., Kang, H. Q., Wang, H. N., and Wang T. J.: Applications of pollutants
961 released from crop residues at open burning in Yangtze River Delta, *Environmental*
962 *Science*, 5, 1418-1424, 2012 (in Chinese).

963 van der Werf, G. R., Randerson, J. T., Giglio, L., Collatz, G. J., Mu, M., Kasi
964 bhatla, P. S., Morton, D. C., DeFries, R. S., Jin, Y., and van Leeuwen, T. T.:
965 Global fire emissions and the contribution of deforestation, savanna, forest, agri
966 cultural, and peat fires (1997-2009), *Atmos. Chem. Phys.*, 10, 11707-11735, doi:
967 10.5194/acp-10-11707-2010, 2010.

968 Van Donkelaar, A., Martin, R. V., Brauer, M., Kahn, R., Levy, R., Verduzco, C., and
969 Villeneuve, P. J.: Global estimates of ambient fine particulate matter concentrations
970 from satellite-based aerosol optical depth: development and application, *Environ.*
971 *Health Persp.*, 118, 847-855, 2010.

972 Vermote, E., Ellicott, E., Dubovik, O., Lapyonok, T., Chin, M., Giglio, L., and
973 Roberts, G.J.: An method to estimate global biomass burning emissions of organic and
974 black carbon from MODIS fire radiative power, *J. Geophys. Res.* 114 (D18)
975 <http://dx.doi.org/10.1029/2008jd011188>, 2009.

976 Wang, S. X., and Zhang, C. Y.: Spatial and temporal distributions of air pollutant
977 emissions from open burning of crop residues in China, *Sciencepaper Online*,
978 5(5):329-333, 2008 (in Chinese).

979 Wiedinmyer, C., Akagi, S. K., Yokelson, R. J., Emmons, L. K., Al-Saadi, J. A.,
980 Orlando, J. J., and Soja, A. J.: The Fire Inventory from NCAR (FINN): a high

981 resolution global model to estimate the emissions from open burning, *Geosci. Model*
982 *Dev.*, 4, 625–641, doi: 10.5194/gmd-4-625-2011, 2011.

983 Wooster, M. J., Roberts, G., Perry, G. L. W., and Kaufman, Y. J.: Retrieval of biomass
984 combustion rates and totals from fire radiative power observations: FRP derivation
985 and calibration relationships between biomass consumption and fire radiative energy
986 release, *J. Geophys. Res.*, 110, D24. <http://dx.doi.org/10.1029/2005jd006318>, 2005.

987 Xia, Y. M., Zhao Y., Nielsen, C. P.: Benefits of China's efforts in gaseous pollutant
988 control indicated by the traditional bottom-up emissions and satellite observations
989 2000-2014, *Atmos. Environ.*, 136: 43-53, 2016.

990 Xiao, Z. M., Zhang, Y. F., Hong, S. M., Bi, X. H., Jiao, L., Feng, Y. C., and Wang, Y.
991 Q.: Estimation of the main factors influencing haze, based on a long-term monitoring
992 Campaign in Hangzhou, China. *Aerosol Air Qual. Res.*, 11, 873-882, 2011.

993 Xing, J., Mathur, R., Pleim, J., Hogrefe, C., Gan, C. -M., Wong, D. C., Wei, C.,
994 Gilliam, R. and Pouliot, G.: Observations and modeling of air quality trends over
995 1990–2010 across the Northern Hemisphere: China, the United States and Europe,
996 *Atmos. Chem. Phys.*, 15, 2723-2747, 2015.

997 Zhang, H. F., Ye, X. G., Cheng, T. T., Chen, J. M., Yang, X., Wang, L., and Zhang, R.
998 Y.: A laboratory study of agricultural crop residue combustion in China: Emission
999 factors and emission inventory, *Atmos. Environ.*, 42, 8432-8441, 2008.

1000 [Zhang, Y., Liu, P., Pun, B., and Seigneur, C.: A comprehensive performance](#)
1001 [evaluation of MM5-CMAQ for the Summer 1999, Southern Oxidants Study](#)
1002 [episode-Part I: Evaluation protocols, databases, and meteorological predictions,](#)
1003 [Atmos. Environ.](#), 40, 4825–4838, 2006.

1004 Zhao Y., Zhang J., and Nielsen C.P.: The effects of recent control policies on trends in
1005 emissions of anthropogenic atmospheric pollutants and CO₂ in China, *Atmos. Chem.*
1006 *Phys.*, 13, 487-508, 2013.

1007 Zheng, Y., Xue, T., Zhang, Q., Geng, G., Tong, D., Li, X. and He, K. B.: Air quality
1008 improvements and health benefits from China's clean air action since 2013, *Environ.*
1009 *Res. Lett.*, 12, 114020, 2017.

1010 Zhou Y., Xing X. F., Lang J. L., Chen D. S., Cheng S. Y., Wei L., Wei X., and Liu C.:
1011 A comprehensive biomass burning emission inventory with high spatial and temporal
1012 resolution in China, *Atmos. Chem. Phys.*, 17, 2839–2864, 2017a.

1013 Zhou, Y. D., Zhao Y., Mao P., Zhang Q, Zhang J., Qiu, L. P., and Yang, Y.:
1014 Development of a high-resolution emission inventory and its evaluation and
1015 application through air quality modeling for Jiangsu Province, China, *Atmos. Chem.*
1016 *Phys.*, 17, 211–233, 2017b.

- 带格式的：字体：Times New Roman
- 带格式的：字体：Times New Roman
- 带格式的：定义网格后不调整右缩进，不调整西文与中文之间的空格，不调整中文和数字之间的空格
- 带格式的：字体：Times New Roman
- 带格式的：检查拼写和语法

1017 **FIGURE CAPTIONS**

1018 **Figure 1. ~~(a) Monthly variations of fire occurrences in 2010 and 2012, (b)~~**
1019 **spatial patterns of fire points in June 2010 and June 2012, ~~(c)~~ PM₁₀**
1020 **concentrations for city-level in YRD in June 2010 and June 2012, and ~~(d)~~**
1021 **temporal variations of daily fire occurrences in June 2010 and 2012. City**
1022 **abbreviations FY, BZ, BB, HN, HF, CZ(a), XZ, LYG, NJ, YZ, ZJ, TZ, NT, CZ,**
1023 **WX, SZ, HZ(a), JX, HZ, SX, NB, SH indicate is Fuyang, Bozhou, Bengbu,**
1024 **Huainan, Hefei, Chuzhou, Xuzhou, Lianyungang, Nanjing, Yangzhou, Zhenjiang,**
1025 **Taizhou, Nantong, Changzhou, Wuxi, Suzhou, Huzhou, Jiaxing, Hangzhou,**
1026 **Shaoxing, Ningbo, and Shanghai).**

1027 **Figure 2. Model domain and locations of 43 meteorological monitoring sites. The**
1028 **numbers of 1-41 represent the cities of Fuyang, Bozhou, Huaibei, Suzhou,**
1029 **Huainan, Bengbu, Luan, Hefei, Chuzhou, Anqing, Chaohu, Maanshan, Chizhou,**
1030 **Tongling, Wuhu, Huangshan, Xuancheng, Xuzhou, Lianyungang, Suqian,**
1031 **Huaian, Yancheng, Yangzhou, Taizhou, Nanjing, Zhenjiang, Nantong,**
1032 **Changzhou, Wuxi, Suzhou; Huzhou, Jiaxing, Hangzhou, Shaoxing, Ningbo,**
1033 **Zhoushan, Quzhou, Jinhua, Taizhou, Lishui and Wenzhou, respectively.**
1034 **~~Model domain and locations of 43 meteorological monitoring sites.~~**

1035 **Figure 3. Fire counts and CO₂ emissions estimated with traditional bottom-up,**
1036 **FRP-based and constraining methods for YRD 2005-2012.**

1037 **Figure 4. Observed 24-hour averaged PM₁₀ concentrations and simulated hourly**
1038 **PM₁₀ concentrations without OBB emissions (No_OBB) and with OBB emissions**
1039 **based on traditional bottom-up (Traditional_OBB), FRP-based (FRP_OBB) and**
1040 **constraining (Constrained_OBB) methods in Lianyungang, Fuyang, Bozhou,**
1041 **Bengbu, Huainan, Hefei, and Chuzhou during June 17-25, 2010.**

1042 **Figure 5. Observed 24-hour averaged PM₁₀ concentrations and simulated hourly**
1043 **PM₁₀ concentrations without OBB emissions (No_OBB) and with OBB emissions**
1044 **based on traditional bottom-up (Traditional_OBB), FRP-based (FRP_OBB) and**
1045 **constraining (Constrained_OBB) methods in Xuzhou, Lianyungang, Fuyang,**
1046 **Bozhou, Bengbu, Huainan, Hefei, and Chuzhou during June 8-14, 2012.**

1047 **Figure 6. Annual CO emissions from OBB in YRD obtained in this work and**
1048 **other studies from 2005 to 2012.**

1049 **Figure 7. Spatial distributions of CO emissions from OBB obtained in this work**
1050 **(constraining method), GFAS v1.0, GFED v3.0 and GFED v4.1s in 2010.**

1051 **Figure 8. The contribution of OBB to PM₁₀ concentrations for different YRD**
1052 **cities during OBB events in June 2010 and 2012.**

1053 **[Figure 9. The contribution of OBB to PM_{2.5} and PM₁₀ concentrations for](#)**
1054 **[different YRD cities during OBB event in June 2014.](#)**

1055 **Figure [9](#)**10. PM₁₀ concentrations contributed by OBB for different YRD cities in**
1056 **Jun 8-14 (PE1) and June 22-28 (PE2), 2012.****

1057 **Figure [10](#)**11. PM₁₀ concentrations contributed by OBB for different YRD cities**
1058 **based on the diurnal variations of 2010 and 2012 in Jun 8-14, 2010.****

1059

1060

TABLES1061 **Table 1. Constrained OBB emissions from 2005 to 2015 in YRD (Unit: Gg).**

	PM ₁₀	PM _{2.5}	EC	OC	CH ₄	NMVOCs	CO	CO ₂	NO _x	SO ₂	NH ₃
2005	175.7	153.7	4.4	38.7	32.1	420.3	670.2	12011.2	22.2	2.7	4.1
2006	171.3	149.9	4.3	37.8	31.3	409.9	653.7	11716.7	21.7	2.6	4.0
2007	219.1	191.7	5.5	48.3	40.0	524.2	835.9	14981.9	27.7	3.4	5.1
2008	176.7	154.6	4.4	39.0	32.3	422.8	674.3	12085.2	22.3	2.7	4.1
2009	178.8	156.4	4.5	39.4	32.6	427.7	682.0	12223.3	22.6	2.8	4.2
2010	257.9	225.7	6.5	58.3	47.6	624.5	987.7	17720.3	33.0	4.0	6.1
2011	188.9	165.3	4.7	41.7	34.5	452.0	720.7	12917.7	23.9	2.9	4.4
2012	389.0	340.4	9.6	83.6	70.2	919.4	1478.6	26473.6	48.6	6.0	9.0
2013	260.7	228.1	6.5	57.5	47.6	623.8	994.7	17828.1	33.0	4.0	6.1
2014	332.4	290.8	8.3	73.3	60.7	795.2	1268.1	22729.0	42.0	5.1	7.8
2015	109.9	96.1	2.8	24.2	20.1	262.9	419.3	7514.6	13.9	1.7	2.6

1062

1063

1064

1065 | **Table 2. Model performance statistics for concentrations of PM_{2.5} and PM₁₀ from**
 1066 | **observation and CMAQ simulation without OBB emissions (No_OBB) and with**
 1067 | **OBB emissions based on traditional bottom-up (Traditional_OBB), FRP-based**
 1068 | **(FRP_OBB) and constraining methods (Constrained_OBB) for the ~~two~~-three**
 1069 | **OBB events of June 2010 ~~and~~, 2012 ~~and~~ 2014.**

			June 2010		June 2012					
			NMB	NME	NMB	NME				
No_OBB			-47%	50%	-60%	68%				
Traditional_OBB			11%	44%	-16%	45%				
FRP_OBB			-33%	41%	-45%	52%				
Constrained_OBB			-16%	37%	-10%	45%				
			No_OBB		Traditional_OBB		FRP_OBB		Constrained_OBB	
			NMB	NME	NMB	NME	NMB	NME	NMB	NME
<u>2010</u>	<u>PM₁₀</u>	<u>Daily</u>	<u>-47%</u>	<u>50%</u>	<u>11%</u>	<u>44%</u>	<u>-33%</u>	<u>41%</u>	<u>-16%</u>	<u>37%</u>
<u>2012</u>	<u>PM₁₀</u>	<u>Daily</u>	<u>-60%</u>	<u>68%</u>	<u>-16%</u>	<u>45%</u>	<u>-45%</u>	<u>52%</u>	<u>-10%</u>	<u>45%</u>
	<u>PM₁₀</u>	<u>Daily</u>	<u>-59%</u>	<u>59%</u>			<u>-54%</u>	<u>54%</u>	<u>-37%</u>	<u>42%</u>
	<u>PM₁₀</u>	<u>Hourly</u>	<u>-59%</u>	<u>60%</u>			<u>-54%</u>	<u>57%</u>	<u>-37%</u>	<u>52%</u>
<u>2014</u>		<u>Daily</u>	<u>-52%</u>	<u>52%</u>			<u>-41%</u>	<u>42%</u>	<u>-12%</u>	<u>39%</u>
	<u>PM_{2.5}</u>	<u>Hourly</u>	<u>-52%</u>	<u>56%</u>			<u>-41%</u>	<u>51%</u>	<u>-13%</u>	<u>54%</u>
<u>Bench</u>	<u>PM₁₀</u>								<u>-45%</u>	<u>49%</u>
<u>-mark</u>	<u>PM_{2.5}</u>								<u>-33%</u>	<u>43%</u>

1070 |
 1071 | Note: ^a from Zhang et al. (2006). NMB and NME were calculated using following equations (*P*
 1072 | and *O* indicate the results from modeling prediction and observation, respectively):

1073 |
$$NMB = \frac{\sum_{i=1}^n (P_i - O_i)}{\sum_{i=1}^n (O_i)} \times 100\% ; NME = \frac{\sum_{i=1}^n |P_i - O_i|}{\sum_{i=1}^n (O_i)} \times 100\% .$$

1074 |

带格式的：上标
 带格式的：非上标/ 下标

1075 **Table 3. OBB emissions in YRD derived from this work and other studies in**
 1076 **2010 (Unit: Gg).**

	PM ₁₀	PM _{2.5}	EC	OC	CH ₄	NMVOCs	CO	CO ₂	NO _x	SO ₂	NH ₃
Traditional (this work)	362.4	317.1	9.3	85.7	67.9	154.9	1391.8	24978.0	47.0	5.4	8.7
FRP-based (this work)	57.8	50.6	6.4	18.5	46.5	412.5	820.1	12718.0	24.9	3.2	17.7
<u>FRP-based (WSE)¹</u>	<u>158.6</u>	<u>139.1</u>	<u>4.1</u>	<u>38.5</u>	<u>30.1</u>	<u>68.7</u>	<u>612.8</u>	<u>11004.3</u>	<u>20.9</u>	<u>2.4</u>	
Constrained (this work)	257.9	225.7	6.5	58.3	47.6	624.5	987.7	17720.3	33.0	4.0	6.1
GFASv1.0	-	17.8	1.0	9.5	15.6	88.7	196.3	3097.8	5.1	1.0	3.1
GFEDv3.0	-	3.5	0.2	1.7	3.2	4.1	39.4	701.6	1.1	0.2	6.4
GFEDv4.1s	-	33.6	4.0	12.4	31.3	53.2	548.3	8519.7	16.7	2.2	11.7
Xia et al, (2016)	350.2	339.3	14.8	137.8	-	-	1989.9	49835.1	134.3	22.6	-

1077 ¹ FRP-based (WSE): the OBB emissions were ~~derived~~estimated with FRP-based method,
 1078 applying ~~the same emission factors as~~ used in the bottom-up method ~~in FRP-based~~
 1079 method ~~and t~~. The emission factors were obtained by weighting emission factors in the
 1080 bottom-up method with the masses of various crop ~~straws of different crop species types~~.
 1081

带格式表格

带格式的：上标

带格式的：正文，左，段落间距段后：0 磅

带格式的：段落间距段前：12 磅，段后：3 磅，行距：多倍行距 1.3 字行

1082
1083
1084
1085
1086

Table 4. The uncertainties of OBB emissions in YRD indicated as 95% CIs and the top two parameters contributing most to emission uncertainties based on traditional bottom-up and FRP-based methods for 2012. The percentages in the parentheses indicate the contributions of the parameters to the variances of emissions.

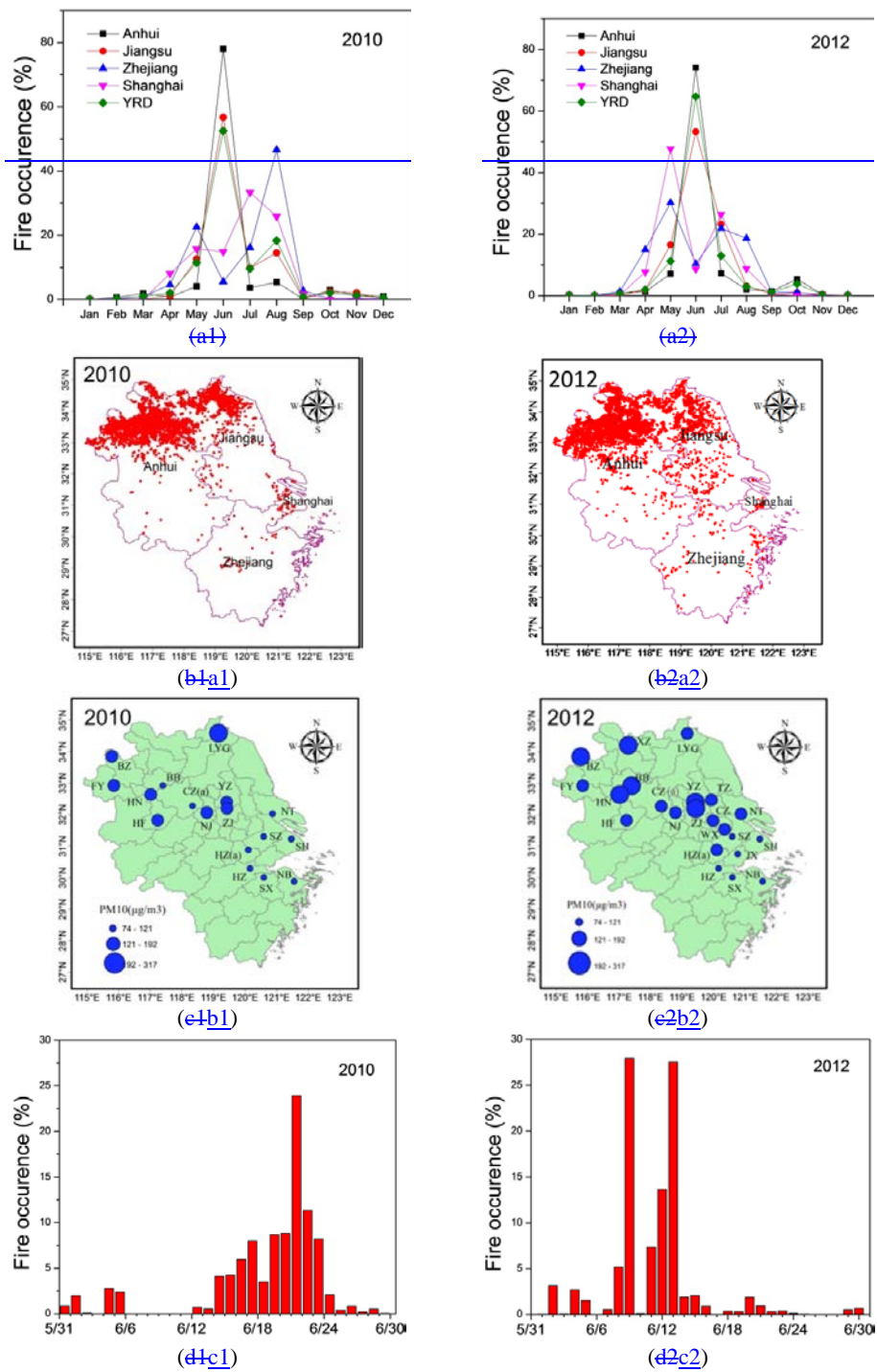
	Traditional bottom-up method		FRP-based method	
PM ₁₀	-56%, +70%	PCRBF ¹ _{Anhui} (42%)	-77%, +274%	EF (76%)
		EF _{wheat} (41%)		AF ² (11%)
PM _{2.5}	-56%, +70%	PCRBF _{Anhui} (43%)	-63%, +244%	EF (65%)
		EF _{wheat} (41%)		NFP ³ (16%)
EC	-50%, +54%	PCRBF _{Anhui} (69%)	-78%, +281%	EF (75%)
		PCRBF _{Jiangsu} (11%)		NFP (11%)
OC	-54%, +73%	PCRBF _{Anhui} (42%)	-78%, +276%	EF (75%)
		EF _{rice} (37%)		NFP (11%)
CH ₄	-49%, +58%	PCRBF _{Anhui} (65%)	-83%, +315%	EF (79%)
		PCRBF _{Jiangsu} (11%)		NFP (9%)
NMVOCs	-48%, +59%	PCRBF _{Anhui} (64%)	-63%, +243%	EF (65%)
		PCRBF _{Jiangsu} (10%)		NFP (16%)
CO	-46%, +73%	PCRBF _{Anhui} (62%)	-52%, +223%	EF (57%)
		PCRBF _{Jiangsu} (10%)		NFP (19%)
CO ₂	-48%, +60%	PCRBF _{Anhui} (69%)	-21%, +164%	NFP (44%)
		PCRBF _{Jiangsu} (10%)		AF (42%)
NO _x	-47%, +87%	PCRBF _{Anhui} (51%)	-82%, +303%	EF (78%)
		EF _{wheat} (23%)		NFP (10%)
SO ₂	-59%, +138%	EF _{wheat} (35%)	-78%, +279%	EF (74%)
		PCRBF _{Anhui} (27%)		NFP (12%)
NH ₃	-51%, +67%	PCRBF _{Anhui} (55%)	-82%, +302%	EF (79%)
		EF _{wheat} (12%)		NFP (10%)

1087
1088
1089
1090

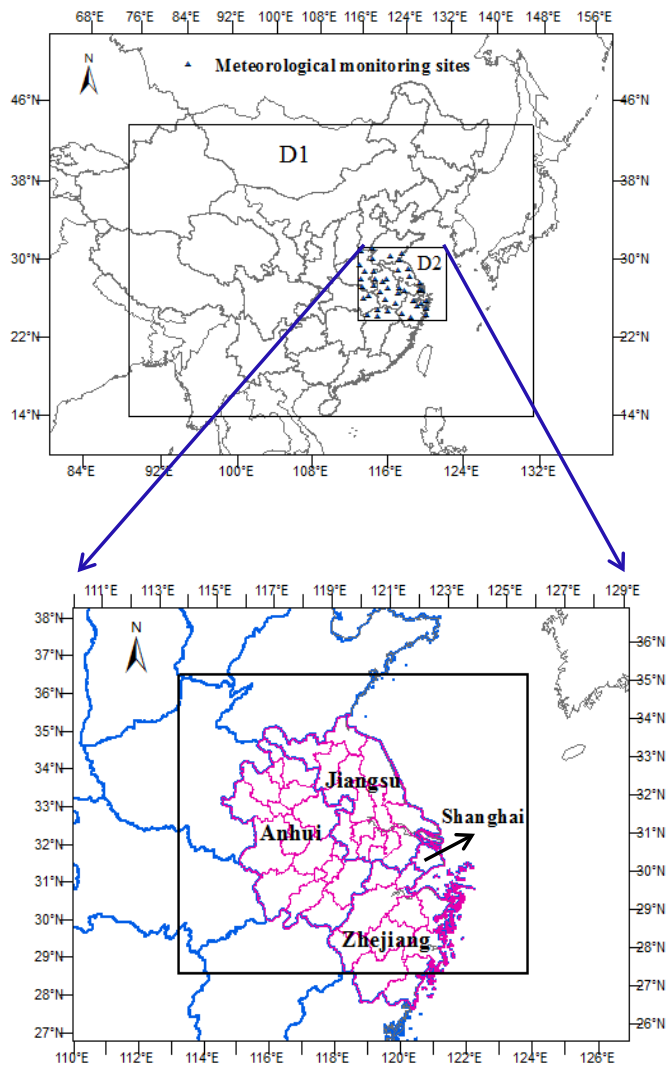
¹ PCRBF, the percentage of crop residues burned in the field (the subscript indicates province); ² AF, the average FRE of fire pixels; ³ NFP, the number of fire pixels; ⁴ MCRBF, the mass of crop residues burned in the field.

带格式的: 字体: Times New Roman, 小四

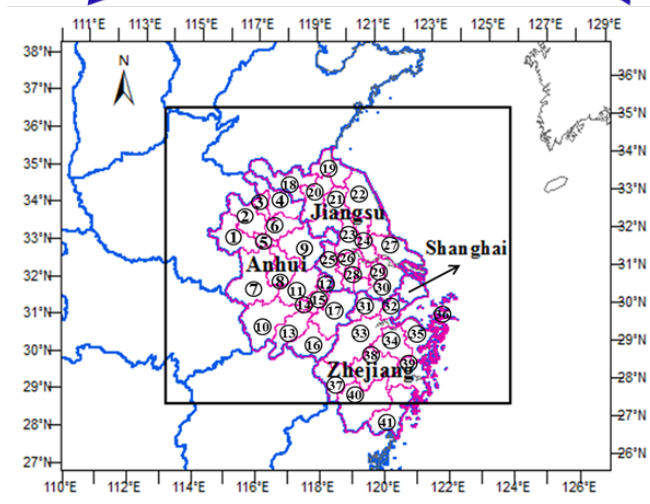
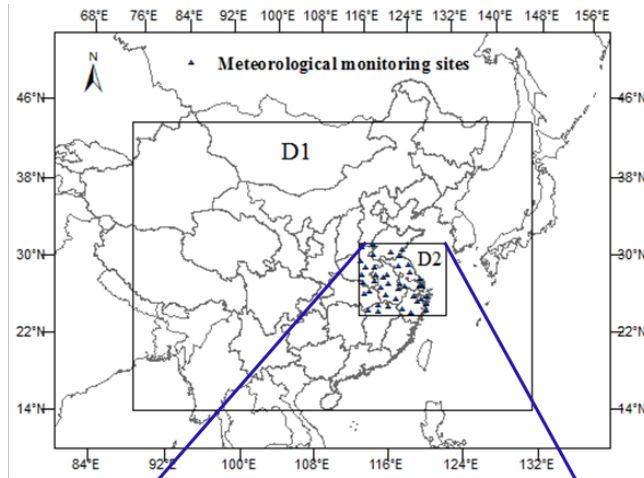
Figure 1.



1093 **Figure 2.**

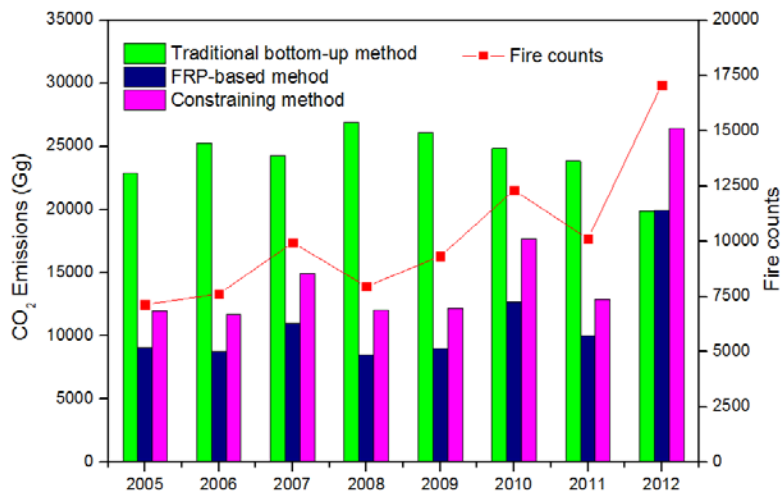


1094



1095
1096

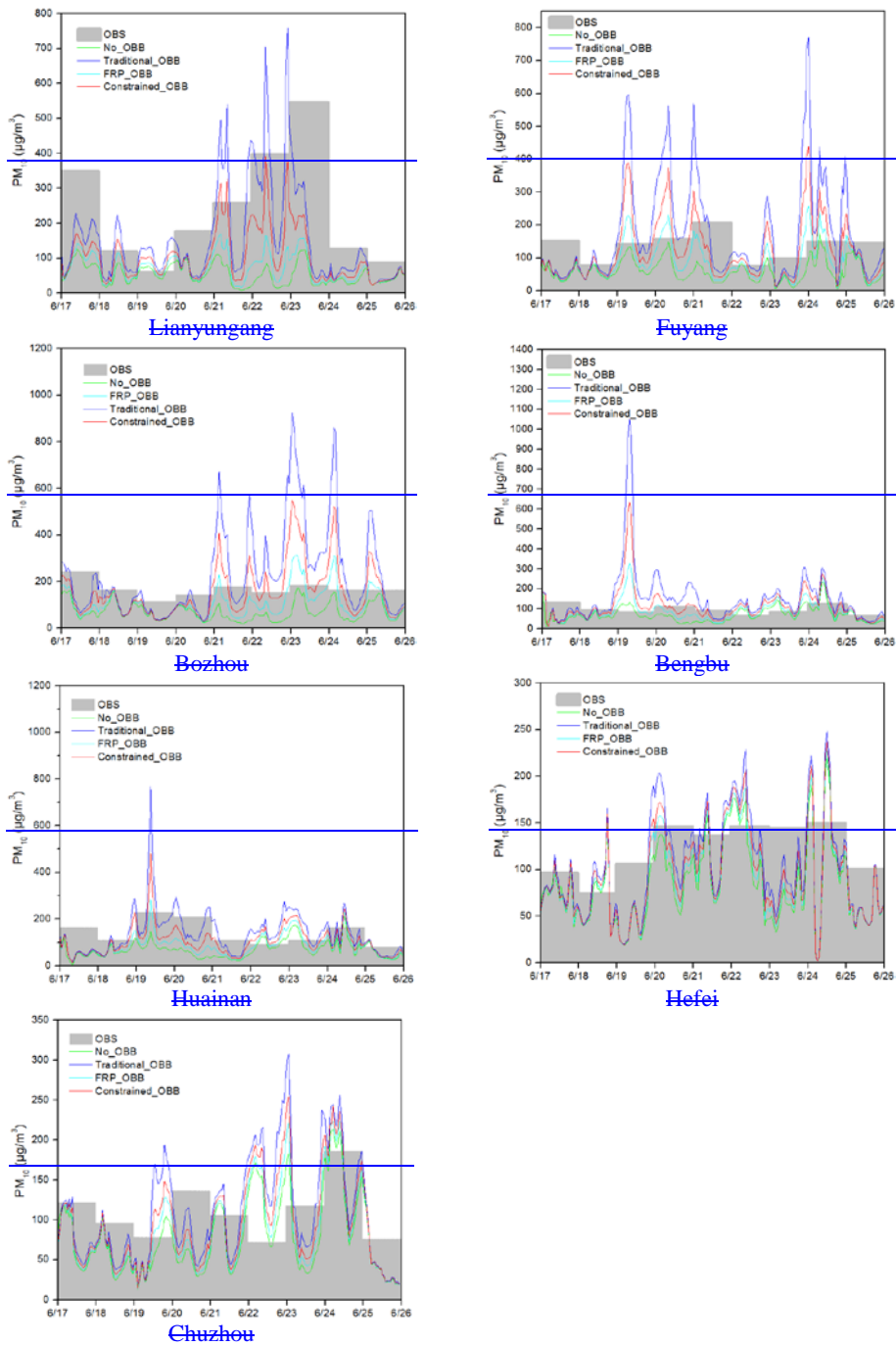
1097 **Figure 3.**

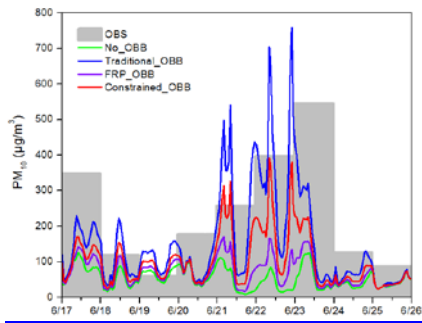


1098
1099

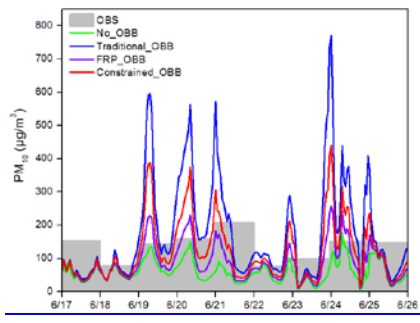
1100

Figure 4.

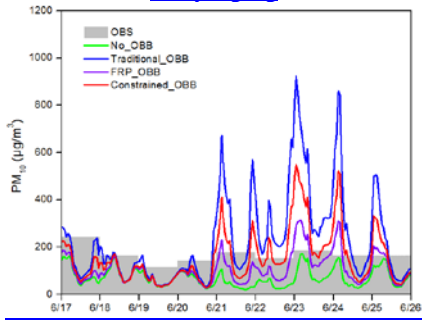




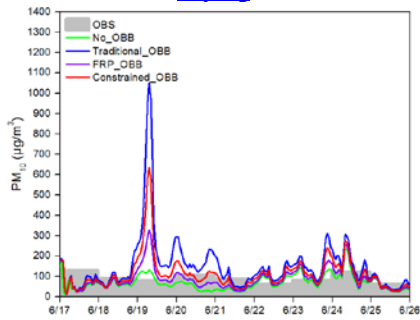
Lianyungang



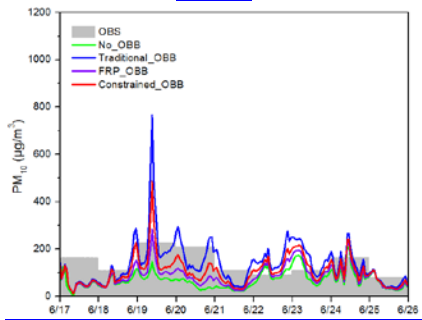
Fuyang



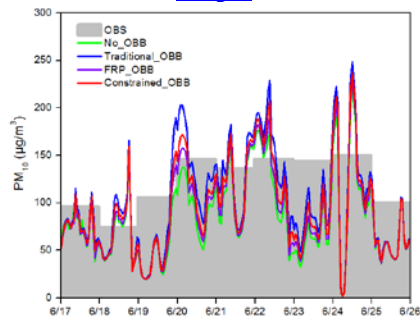
Bozhou



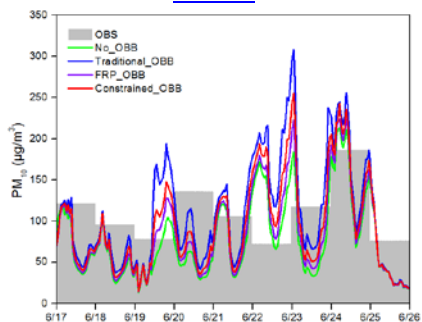
Bengbu



Huainan



Hefei

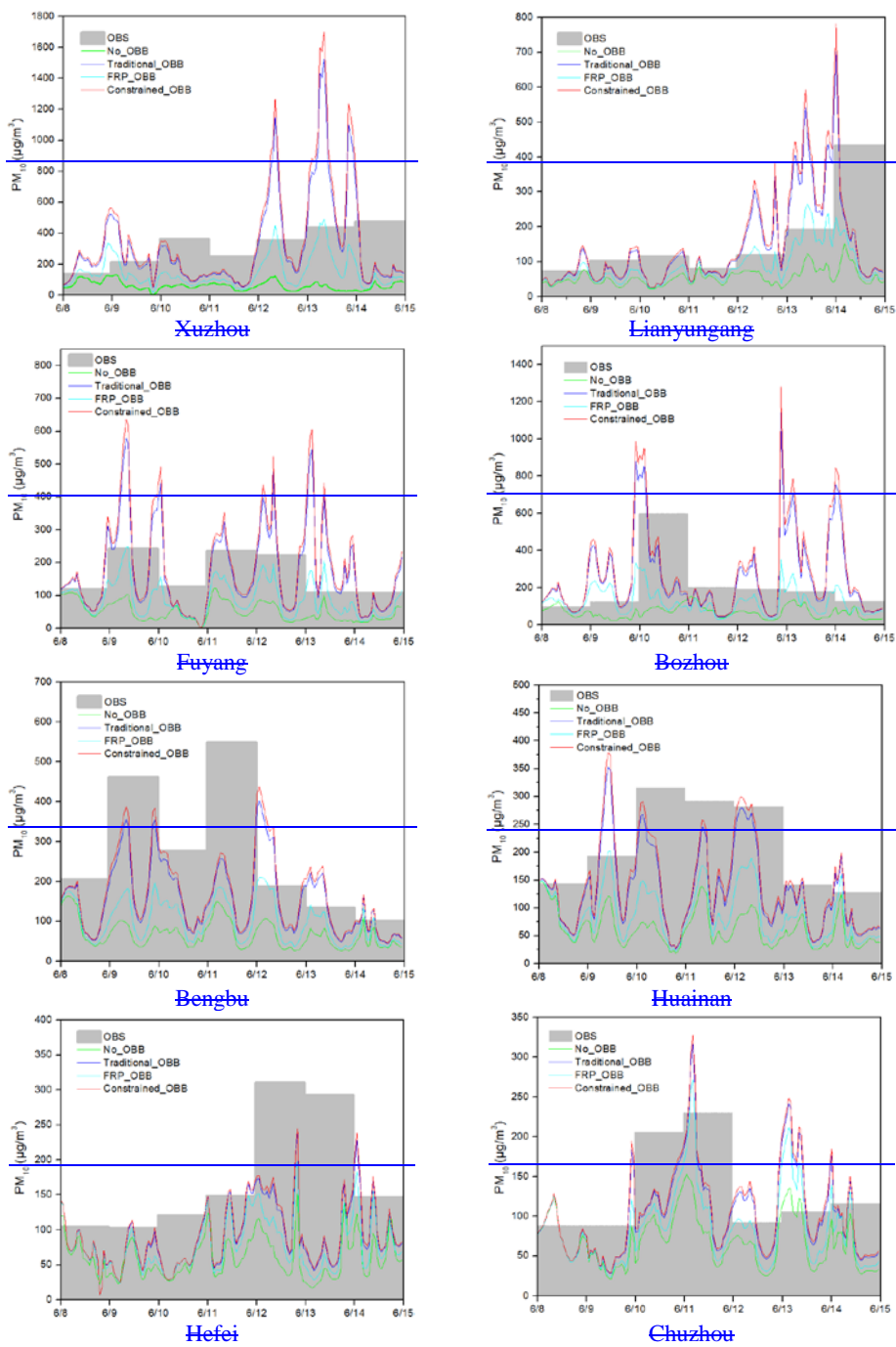


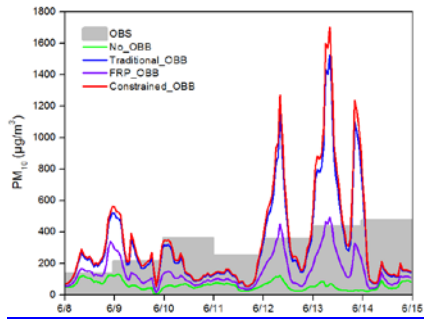
Chuzhou

1102

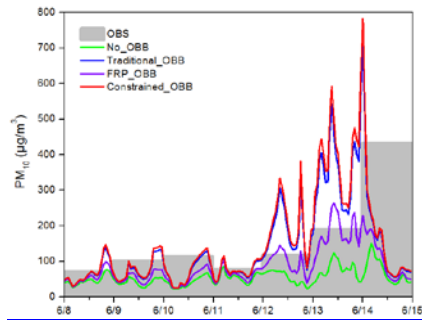
1103

Figure 5.

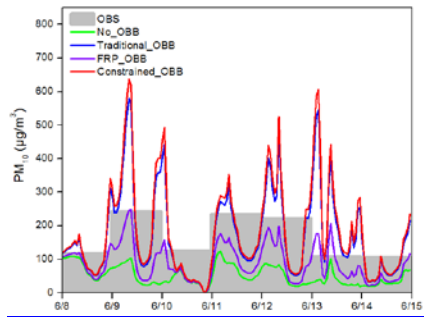




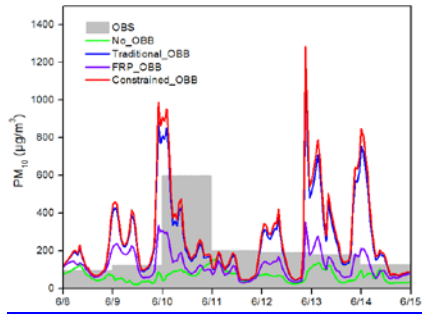
Xuzhou



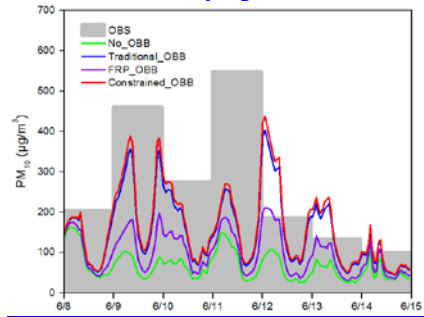
Lianyungang



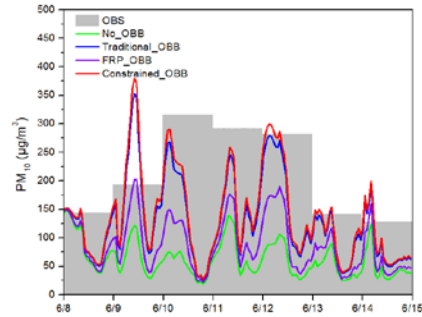
Fuyang



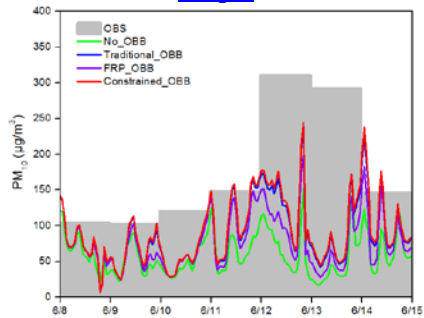
Bozhou



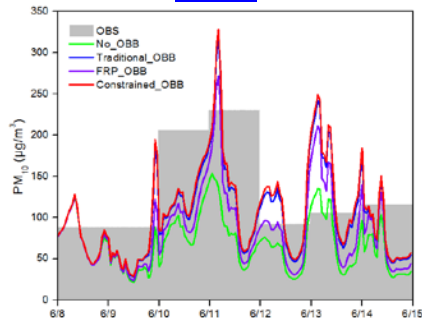
Bengbu



Huainan



Hefei

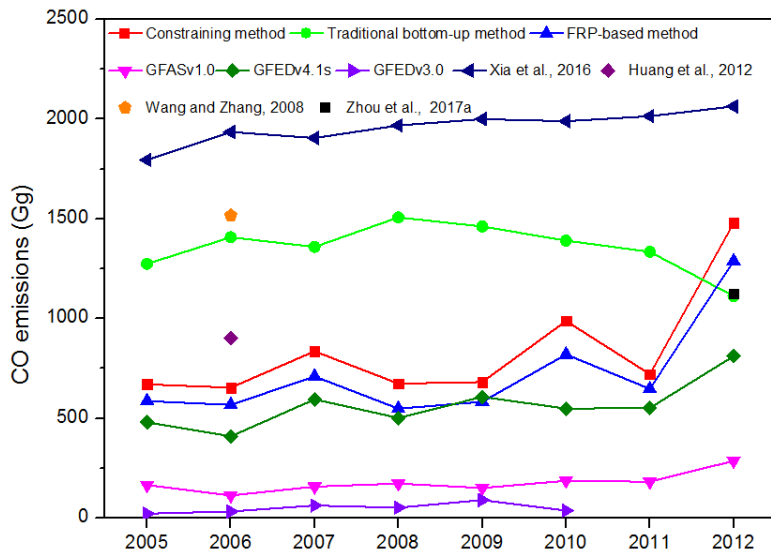


Chuzhou

1105

1106

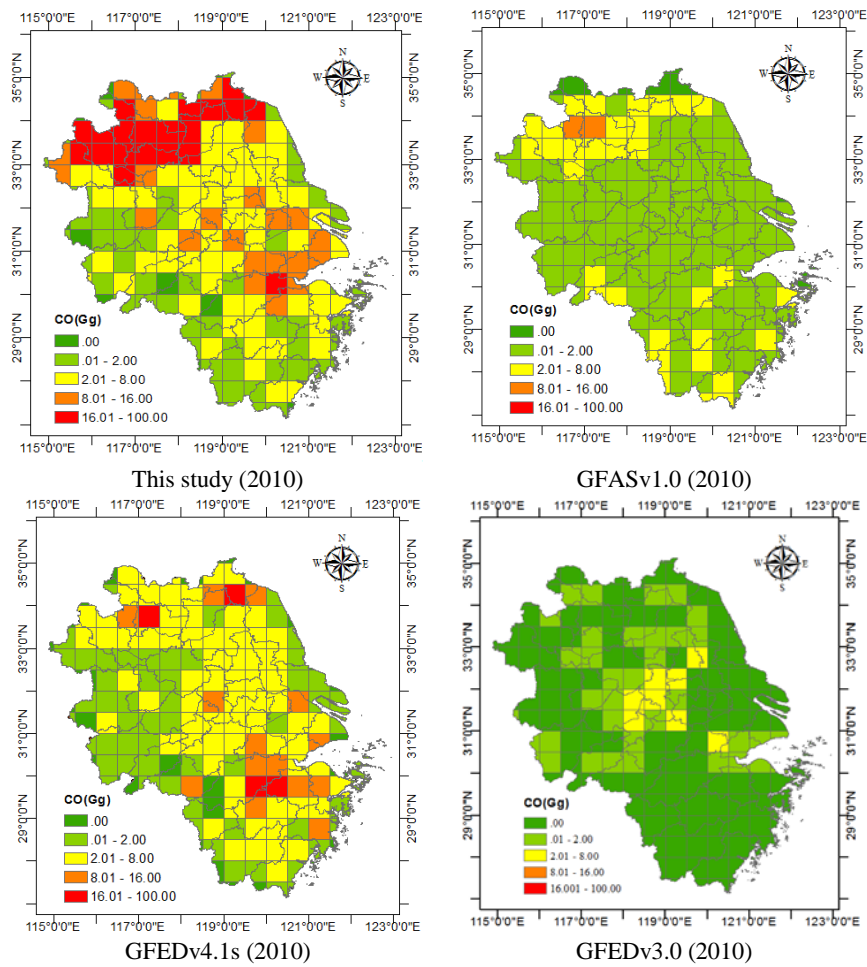
1107 **Figure 6.**



1108

1109

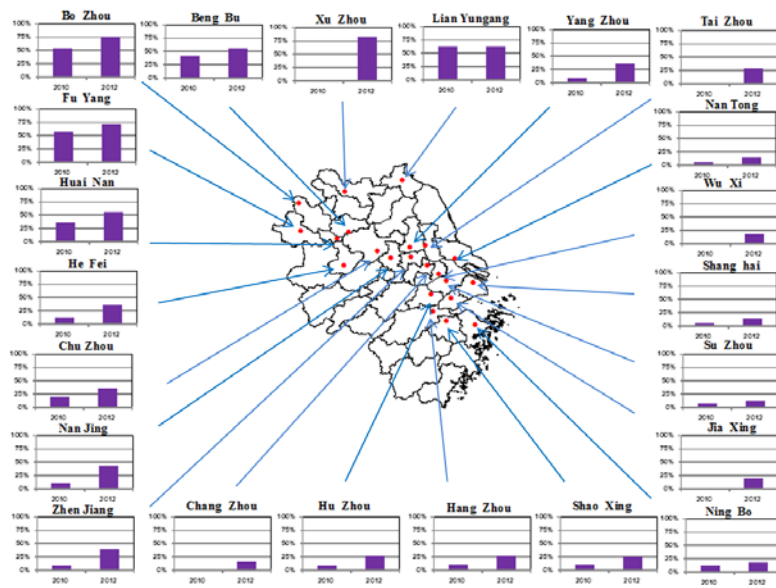
1110 **Figure 7.**



1111

1112

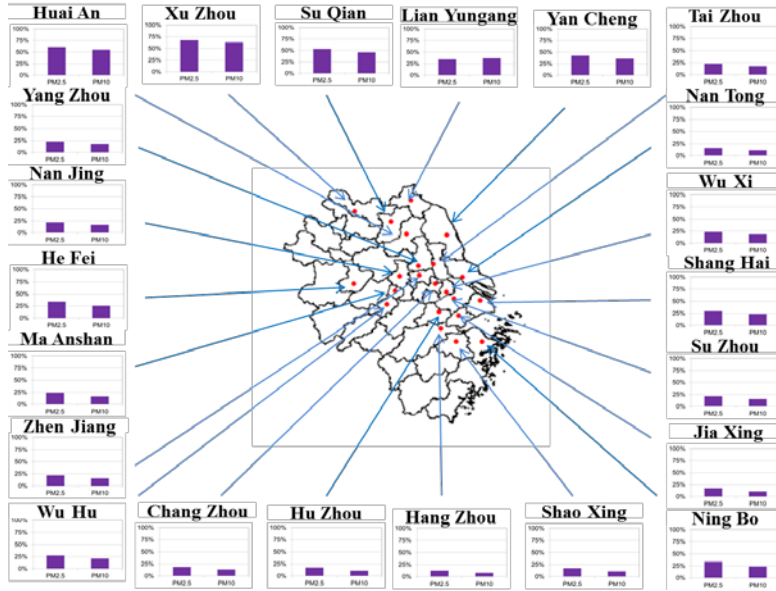
1113 **Figure 8.**



1114
1115

1116

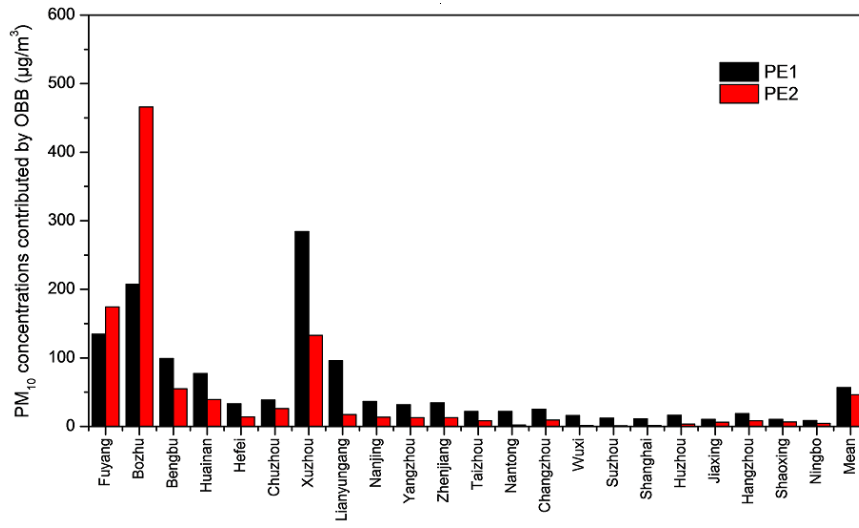
Figure 9.



1117

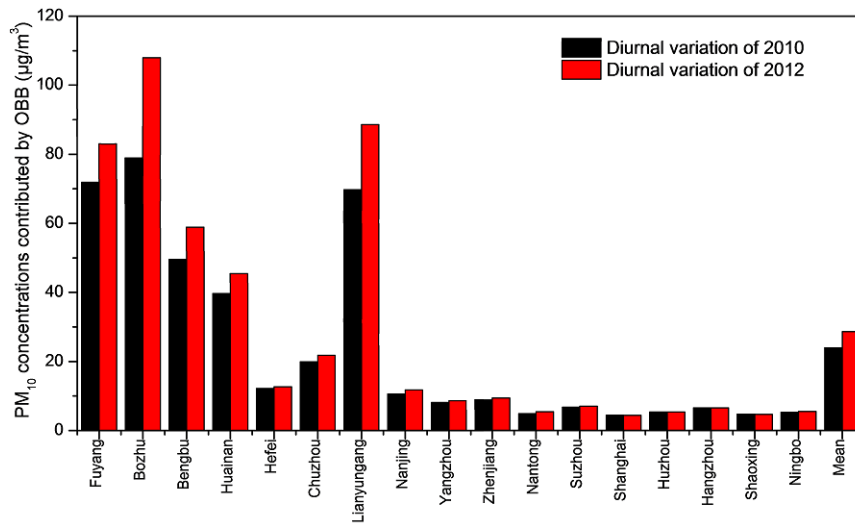
1118

1119 | **Figure 910.**
1120



1121
1122

1123 | **Figure 1011.**



1124